



National Institute for Public Health
and the Environment
Ministry of Health, Welfare and Sport

**Predicting the dispersion and
deposition of particles released in a fire**
Minor Research Project
Toxicology & Environmental Health Report 261
Joris Meesters



Colofon

© RIVM 2011

Parts of this publication may be reproduced, provided acknowledgement is given to the 'National Institute for Public Health and the Environment', along with the title and year of publication.

J.A.J. Meesters (Intern), RIVM

Contact:

P.A.M. Heezen

RIVM

patrick.heezen@rivm.nl

This investigation has been performed by order and for the account of RIVM / Institute of Risk Assessment Sciences (IRAS), within the framework of Centre for External Safety

Abstract

Predicting the dispersion and deposition of particles released in a fire

During a fire soot particles are formed which may contain hazardous substances such as PAHs, dioxins and heavy metals. These particles disperse through the air and deposit on the ground. To give advice concerning public health the Centre for External Safety (CEV) predicts the particle dispersion and deposition during and after the fire. The CEV however recognizes significant uncertainties in the used assumptions and model. The influence of these uncertainties on the final prediction was analyzed. Major uncertainties are the height of the smoke plume, the emission rate of particles and the particle size distribution. For a well-constructed health advice model results alone do not suffice, measurements are necessary also.

Keywords: Modelling, Fire, Particle, Dispersion, Deposition

Rapport in het kort

Het voorspellen van dispersie en depositie van deeltjes die vrijkomen bij een brand

Tijdens een brand ontstaan roetdeeltjes die gevaarlijke stoffen zoals PAKs, dioxinen en zware metalen kunnen bevatten. Deze deeltjes verspreiden zich door de lucht en slaan neer op de grond. Om tijdens en na een brand een advies in het kader van de volksgezondheid te kunnen geven, worden de verspreiding en depositie van de deeltjes voorspeld door het Centrum voor Externe Veiligheid (CEV). Het CEV erkent echter grote onzekerheden in het model en de aannames die gebruikt worden. Er is een analyse gedaan naar de invloed van deze onzekerheden op de voorspelling. De grootste onzekerheden zijn gerelateerd aan de stijghoogte van de rookpluim, de emissie van het aantal deeltjes per seconde en de verdeling van de grootte van de deeltjes. Voor een goed onderbouwd advies zijn naast modelresultaten metingen noodzakelijk.

Trefwoorden: Modelleren, Brand, Deeltjes, Dispersie, Depositie

Contents

Summary—8

Glossary—10

1. Introduction—14

- 1.1 Research motive—14
- 1.2 Research goal—14
- 1.3 Global approach—15

2 Methods for literature research—16

- 2.1 Review of all parameters and processes—16

3 Basic chemistry and physics of fire—18

- 3.1 The role of fuel and heat in a fire—18
- 3.2 The role of the oxygen level in a fire—19
- 3.3 The role of chain reactions, mixing and proportioning in a fire—19
- 3.4 Fire transfer and stages in fire development—19
 - 3.4.1 Fire transfer through conduction—19
 - 3.4.2 Fire transfer through convection—19
 - 3.4.3 Fire transfer through radiation—19
 - 3.4.4 Fire transfer through direct flame contact—20
 - 3.4.5 Incipient stage in fire development—20
 - 3.4.6 Free-burning stage in fire development—20
 - 3.4.7 Smoldering stage—21

4 Formation of particles in smoke production—22

- 4.1 Particle formation in pyrolysis and smoldering combustion—22
- 4.2 Particle formation in flaming combustion—23
- 4.3 Particle yield—24
- 4.4 Particle size distribution—24

5 Smoke plume dispersion trajectory—26

- 5.1 Atmospheric stability—27
- 5.2 Plume rise—29
- 5.3 Passive dispersion by the commonly used Gaussian Plume Model (GPM)—31
- 5.4 Atmospheric boundary layer and mixing height—32

6 Atmospheric deposition—33

- 6.1 General dry deposition of materials—33
- 6.2 Dry deposition of particles—33
- 6.3 General wet deposition of materials—35
- 6.4 Wet deposition of particles—35

7 Toxicity of fire released airborne particles and particle bound substances—36

- 7.1 Measurements of particulate matter and particle bound substances at fire sites in the Netherlands—36
- 7.2 Toxicity of airborne particles—37
 - 7.2.1 Toxicity of airborne particles—37
- 7.3 Polycyclic aromatic hydrocarbons (PAHs)—39
 - 7.3.1 Toxicity of PAHs—39

7.3.2	Fire conditions affecting PAH emissions—40
7.4	Dioxins—40
7.4.1	Toxicity of dioxins—40
7.4.2	Fire conditions affecting dioxin emissions—41
7.5	Heavy metals and airborne metals—42
8	Literature research conclusions—43
9	CEVs' Current method in predicting the dispersion and deposition of particles released in a fire—46
9.1	Fire conditions—46
9.1.1	PGS-15 fires—46
9.1.2	Miscellaneous fires—46
9.2	Deriving PHAST input data—47
9.2.1	Source emission input data—47
9.2.2	Building dimensions input data—49
9.2.3	Atmospheric stability and wind input data—50
9.3	Deriving deposition formula variable values from PHAST output—51
9.4	Calculation of particle deposition—53
9.5	Flow chart of CEV-method—54
9.6	Additional remarks by the CEV—54
10	Critical review on the CEV-method—55
10.1	Scientific background on deposition variable assumptions—55
10.1.1	Deposition velocity, dry deposition—55
10.1.2	Scavenging rate, wet deposition—56
10.2	Parameters that are not (directly) included in the CEV-method—57
10.3	Indicative verification—58
11	Sensitivity analyses: used models and methods—61
11.1	Model selection for parameters particle size distribution, plume rise and inversion layer height: OPS- Short Term—62
11.2	Sensitivity analyses with PHAST—63
11.2.1	Default input values—63
11.2.2	Downwind deposition flux profiles—65
11.3	Sensitivity analysis with OPS-ST—66
11.3.1	Default input values—66
11.3.2	Downwind deposition flux profiles—67
12	Sensitivity analyses performed with PHAST—68
12.1	Release rate—68
12.2	Pre-dilution air rate—69
12.3	Final release temperature—70
12.4	Atmospheric stability and wind speed—71
12.5	Building dimensions—73
13	Sensitivity analyses performed with OPS-ST—75
13.1	Plume rise—75
13.1.1	Inserted values—77
13.1.2	Dry deposition flux profiles for different plume rise heights—78
13.2	Particle size distribution—79
14	Discussion—81
14.1	Consequences of input uncertainty for parameters—81
14.1.1	Release rate—81

- 14.1.2 Building dimensions—81
- 14.1.3 Pre-dilution air rate—81
- 14.1.4 Final release temperature—81
- 14.1.5 Atmospheric stability—82
- 14.1.6 Plume rise—82
- 14.1.7 Particle size distribution—82
- 14.2 No sensitivity analyses on source term parameters—84
- 14.3 No sensitivity analyses performed on inversion layer height—84
- 14.4 Personal interpretation in choosing concentration layer values for PHAST sideview graphs—84
- 14.5 Release of heavy metals in fires—84
- 14.6 Nanosized particles released in a fire—84
- 14.7 Soil contamination by PAHs and dioxins bound to deposited particles—85

15 Conclusion—86

- 15.1 The CEV-method—86
- 15.2 Critical review on the CEV-method—87
- 15.3 Uncertainties and their consequences—87
- 15.4 Answer on the research question—88

16 Recommendations—89

- 16.1 Recommendations for CEV-method improvement—89
 - 16.1.1 No reasons to believe the CEV-method is mathematically incorrect—89
 - 16.1.2 No prediction in case of visually observed plume rise—89
 - 16.1.3 Deposition flux tool in PHAST—89
- 16.2 Recommendations for further research—89
 - 16.2.1 The interaction between plume rise and inversion layer height—89
 - 16.2.2 Size distribution of particles formed in a fire—90
 - 16.2.3 Modelling source term parameters with FIREPEST—90

17 Literature—91

Summary

Research motive

During a fire particles (soot) are released which may contain hazardous substances such as polycyclic aromatic hydrocarbons (PAHs), dioxins and heavy metals. These particles will disperse through air and then deposit to the ground. For the assessment of health effects it is important to estimate the concentration of these substances in the air and on the ground. The polluted air is important for human exposure because inhalation is an important exposure pathway. Deposition of particles could result in contamination of crops and grass eaten by livestock introducing the dioxins, PAHs and heavy metals in the food chain. During or after a fire the Centre for External Safety (CEV) is often asked to predict particle dispersion and deposition caused by the fire, but only simple assumptions are available for this prediction. The CEV therefore wishes to improve its method. The aim of this study is to retrieve the uncertainties by modelling the particle dispersion and deposition, to determine the influence of these uncertainties, and to give recommendations.

Methods

Based on a literature study, expert interviews and a critical review of the CEV-method it has been determined what parameters are important in predicting the dispersion and deposition of particles released in a fire. The major parameters for the CEV-method are 'release rate', 'building dimensions', 'pre-dilution air rate', 'final release temperature', and 'atmospheric stability'. Parameters that are not or only indirectly included in the CEV-method are 'plume rise' and 'particle size distribution'. Sensitivity analyses have been performed for all the mentioned parameters, in order to determine their influence on the predicted deposition. The major parameters in the CEV-method have been analysed with the model PHAST. The parameters 'plume rise' and 'particle size distribution' have been analysed with the air dispersion model OPS-ST.

Conclusions

The results show that most uncertainty is caused by the parameter 'plume rise'. During a fire a smoke plume rises and the height is an important parameter to predict the particle deposition flux. This plume rise height is difficult to measure and cannot be predicted with the currently available models. The sensitivity of plume rise height is especially strong when predicting particle deposition close to the fire (0-100m) and between relatively low plume rise heights. In the CEV-method the plume rise height is assumed to be zero, which in general leads to an overestimation of particle deposition.

The amount of particles that is released in the air 'the release rate' is another parameter causing major uncertainty. With the available data it is very difficult to predict the amount and exact type of particles released in the atmosphere per second. The uncertainty in release rate is linear to the uncertainty in the final prediction. However the uncertainty is still major because release rate is a very important parameter.

A third important uncertainty is the size distribution of the particles formed in the fire. The parameter 'particle size distribution' cannot be predicted based on the fire conditions and the present fuels, but scientific literature provides some indications for assuming a size distribution typically for particles formed in a fire. Particles formed in a fire are typically larger, than particles in general air pollution study. If a relative large mass-fraction of large particles ($> 20\mu\text{m}$) is

formed, the particles will deposit faster. The CEV-method deals with this uncertainty by assuming that this speed of depositing particles is within a certain range. Sensitivity analyses indicate the true deposition velocity is within this range, but it increases uncertainty of the predicted deposition concentration with a factor 10.

Recommendations for CEV

The prediction method that the CEV applies seems rather unorthodox, but within the scope of this study there are no reasons to believe the CEV-method is incorrect. The applied deposition formulas are acknowledged in scientific literature. The calculated deposition flux values based on the output of the consequence and risk model PHAST are comparable with the deposition flux values that are modelled with air dispersion model OPS-ST. Also an indicative verification provides no reason to believe that the CEV-method is mathematically incorrect.

The general CEV-approach not to perform calculations in case of visually observed plume rise seems valid. In case of a relative large plume rise particle concentrations at residential height are strongly diluted. Moreover the sensitivity of plume rise causes major uncertainty on the calculation outcomes.

The CEV-method predicts deposition flux by performing calculations based on PHAST output. Based on the sideview graphs the values for the necessary variables 'concentration at 1 m height' and 'air column content' are determined by a personal interpretation. This would not be necessary, if a tool is introduced in PHAST that calculates deposition directly from the sideview. With this tool the CEV-method takes less time, is more accurate and is easier to perform.

Glossary

ABL	atmospheric boundary layer
aerodynamic diameter	diameter of a spherical particle that has the same free-fall velocity as the arbitrarily shaped particle
aerosol	airborne particle
agglomeration	fusion of primary particles
atmospheric stability	the extent to which vertical temperature (= density) gradients promote or suppress turbulence in the atmosphere
BOT-mi	cooperation of multiple governmental organisations, which alarms, informs, advises and communicates in case of a calamity with hazardous substances to the competent authority
buoyancy	the upward force (Archimedes force) that is caused by a cloud or plume in which the density is lower than the surrounding atmosphere
CEV	Centre for External Safety
coagulation	particle growth through particle-particle collisions
condensation	particle growth through vapors condensing on the surface of the particle
conduction	transfer of heat via direct contact through a solid body
convection	transfer of heat caused by changes in density in liquids and gases
density	specific weight
deposition	absorption of gas or particles by the ground or vegetation
dispersion	mixing and spreading of gases in air
dry deposition	no-precipitation mediated deposition of particles on the ground
flamepoint	the lowest temperature in which the fuel produces enough vapour to sustain a continuous flame
flaming combustion	combustion of fuel by continuous flames

flashpoint	the lowest temperature in which a liquid or solid material produces enough vapour to burn
free-burning stage	stage in which a fire intensifies and is spreading upward and outward via conduction, convection, radiation and direct flame contact
Gaussian plume model	Langrangian model describing dispersion over short distances from the source (maximum 30km) assuming that turbulence is a random process, it is expected that the mean concentration of material emitted from a point source will have a two-dimensional Gaussian distribution perpendicular to the mean wind direction
geometric average	a type of mean or average, which indicates the central tendency or typical value of a set of numbers. It is similar to the arithmetic mean, except that the numbers are multiplied and then the nth root (where n is the count of numbers in the set) of the resulting product is taken
geometric standard deviation	describes how spread out are a set of numbers whose preferred average is the geometric average
GPM	Gaussian plume model
ignition temperature	also referred to as auto ignition point, the temperature at which the vapour will ignite without a spark
incipient stage	beginning fire with localized flames
LFL	lower flammability limit
mixed layer	layer below the mixing height
mixing height	height of the turbulent boundary layer over the ground
MOD	Environmental Accident Service
Monin-Obukhov length	length-scale which characterizes the atmospheric stability
neutral atmosphere	atmosphere where potential temperature is constant with height
OPS	Operational Priority Substance model
OPS-ST	Version of the OPS-model for short term modeling
PAH	Polycyclic Aromatic Hydrocarbon
particle yield	the percentage of the mass of a burning material which is converted into particles

passive dispersion	dispersion solely caused by atmospheric turbulence
Pasquill-Gifford curve	expressions are developed by Gifford in order to correlate the vertical dispersion coefficient and horizontal dispersion coefficient with atmospheric variables based on the Pasquill stability classes
PHAST	a software package for consequence modelling of accidental releases of toxic or flammable chemicals to the atmosphere, used in CEV's current method
plume rise	the ascent of a plume in the air due to vertical momentum at the source or buoyancy
precipitation	rain, snow, etc.
primary particles	the smallest soot particles grown from PAH-molecules
pyrolysis	the combustion of materials due to a sufficient external source of heat enabling to cause the material to burn without a flame
radiation	transfer of heat by infrared radiation (heat waves) with no material substances involved
rain-out	absorption of gas or particles in rain-drops inside a rain cloud
Richardson number	the flux of the Richardson number is the ratio between the production of kinetic energy by (heat-induced) buoyancy and the production of kinetic energy by mechanical turbulence velocity
scavenging rate	rate of the travelling of a particle until it is taken up by a rain drop
sedimentation	the deposition of particles on the ground due to their free-fall velocity
smoldering	the transformation of a compound into one or more other substances by heat alone
smoldering stage	stage in which the fire is contained and oxygen levels are below 15 to 16%
stable atmosphere	atmosphere where potential temperature increases with height
turbulence	random motions in a fluid due to instabilities of a large-scale flow
UFL	upper flammability limit, above this concentration too little oxygen is available to maintain combustion

unstable atmosphere	atmosphere where potential temperature decreases with height
Von Karman constant	proportionality constant appearing in the relation between velocity gradient and shear stress for turbulent flow near a rough surface
wash-out	absorption of gas or particles in rain-drops falling through a gas cloud or plume beneath a rain cloud
wet deposition	the sum of rain-out and wash-out
x_f	horizontal distance between source emission and maximum plume rise

1. Introduction

1.1 Research motive

During a fire (soot) particles are released which possibly contain hazardous substances such as polycyclic aromatic hydrocarbons (PAHs), dioxins and heavy metals. These particles will disperse through the air and then deposit to the ground. For health reasons it is important to estimate the concentration of these substances in the air and on the ground. Inhalation of the particles in the air is an important exposure mechanism for humans. Respiration of small particles, containing heavy metals and PAHs, has been associated with various health effects (EEA, 2009). Livestock and crops need to be protected against the contaminated soil. An exposure route of PAHs and dioxins through the food chain has been associated with carcinogenic effects (WHO, 2000; WHO 2010)

The Dutch National Institute of Public Health and Environment (RIVM) has a knowledge centre specialized in the assessment of the risk of storage and transport of dangerous substances: The Centre of External Safety (CEV). The CEV is part of the Dutch Environmental Incidents Policy Supporting Team (BOT-mi). The BOT-mi is a cooperation of multiple governmental organisations, which alarms, informs, advices and communicates the competent authority in case of a calamity with hazardous substances. During fire incidents the BOT-mi cooperation frequently has asked the CEV to predict the dispersion and deposition of the hazardous particles released in a fire, so that BOT-mi is able to construct an advice for the protection of crops and livestock against PAHs, dioxins and heavy metals. The CEV recognizes uncertainties in their prediction methodology because it uses simple assumptions. The CEV wishes to improve their modelling methods in order to be able to give more accurate predictions for the construction of the BOT-mi-advice.

The CEV have therefore constructed an internship research project for a Utrecht University master student to examine the possibilities of method improvement over the period of December 2010 till June 2011.

1.2 Research goal

The CEV wishes to improve their methods in predicting the deposition and dispersion of particles released in a fire. In order to assess the possibilities for method improvement the uncertainties when predicting particle dispersion and deposition must be recognized. The aim of this study is to retrieve these uncertainties and to determine the consequences of these uncertainties on the prediction applying the current CEV-method. The main research question therefore is:

“What are the consequences of the uncertainties in predicting dispersion and deposition of particles released in a fire when using the current CEV-method?”

1.3 Global approach

The CEV recognizes uncertainties in their method to predict dispersion and deposition of particles released in a fire. The aim of this study is to find out what these uncertainties are and to determine the consequences of these uncertainties on the prediction. In order to reach this aim a study has been designed with several steps.

First a literature study and expert interviews have been performed in order to create an overview of all parameters and processes contributing in the dispersion and deposition of particles released in a fire. Secondly the current method the CEV applies has been described. By comparing the CEV-method with the outcomes of the literature study it has been determined what parameters are not or only indirectly included in the CEV-method. These 'missing' parameters have been added to the uncertainties already recognized by the CEV-method.

Next the consequences of all uncertainties have been assessed by performing sensitivity analyses for the most important parameters used in the CEV-method and parameters that are believed to be relevant according to the literature study. The results of the sensitivity analyses show the influence of a parameter on the final prediction of particle dispersion and deposition. Based on the sensitivity and uncertainty of the parameters it has been discussed what the consequences of the uncertainties are.

2 Methods for literature research

2.1 Review of all parameters and processes

The dispersion and deposition of particles released in a fire is considered as an environmental process with the basic structure:

Source → Environmental pathway → Effects on human and environment

In order to review all parameters and processes contributing to the dispersion and deposition of particles released in a fire an interpretation of this basic structure has been made, see figure 1.

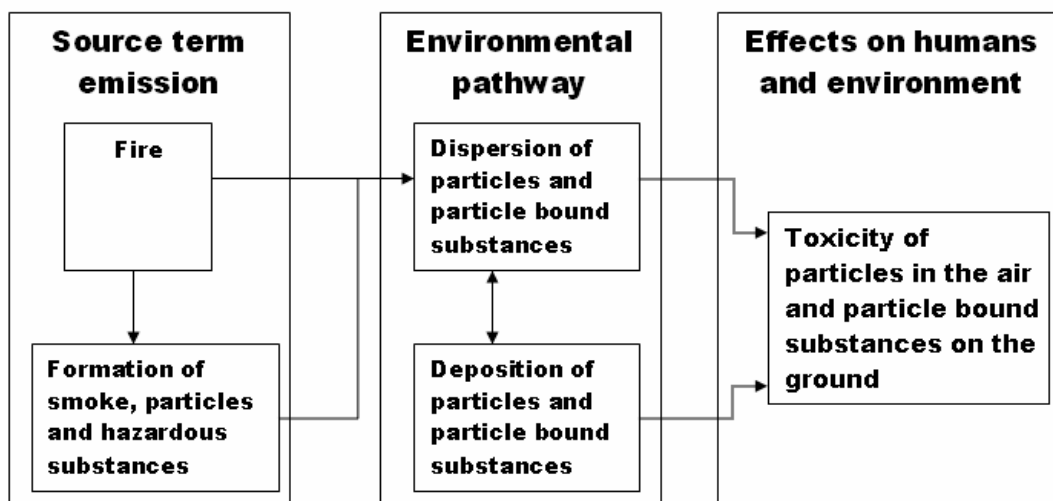


Figure 1. Interpretation of environmental model for the dispersion and deposition of particles released in a fire: 3 steps and 5 processes.

Figure 1 is a relative simple representation of the trajectory of the formation, dispersion and deposition of particles released in a fire. In reality the trajectory is much more complex with many parameters and processes influencing each other directly or indirectly (Mennen et al, 2009). Therefore a literature study and experts interviews have been performed for the 5 main processes displayed in figure 1. The aimed results are a description of all parameters, (sub) processes and their influences on each other. A parameter is defined as a variable determining the state of a process or system and can be expressed in units. A process cannot be expressed in units and is defined as an interaction of (input) parameters resulting into new (output) parameters. The consulted literature consists of scientific articles and books and the following experts have been interviewed:

- Drs. ing. Jurgen van Belle (RIVM), project leader in the division that performs field measurements in case of an accident with hazardous materials (like a large fire) within the Environmental Accident Service (MOD)
- Dr. ir. Addo van Pul (RIVM), expert in the dispersion and deposition of particles in the environment within the Centre of Environmental Monitoring (CMM)
- Dr. Flemming Cassee (RIVM), expert in health effects of particulate matter within the Centre of Environment, Health, and Environmental Quality (MGO)
- Ir. Ferd Sauter (RIVM), expert in the dispersion and deposition of particles in the environment within the Centre of Environmental Monitoring (CMM)
- Dr. Arjan van Dijk (RIVM), expert in the modelling of the environmental impact of nuclear incidents for the Laboratory of Radiation Research Department (LSO). He performed the environmental modelling of the smoke plume dispersion of the Moerdijk fire on January the 5th of 2011.
- Dr. ir. Jos Post (NIFV), manager of the research department of the National Institute for Physical Safety (NIFV)
- Dr. Joost Wesseling (RIVM), expert in the dispersion and deposition of particles in the environment within the Centre of Environmental Monitoring (CMM)
- Jeroen van Leuken, MSc (RIVM), Phd student in modelling Q-fever as a consequence of particle dispersion and deposition with OPS.

3 Basic chemistry and physics of fire

Fire combustion reactions consist of elements heat, oxygen, fuel and chain reactions. The basic physic and chemical principles of a fire can be explained by a tetrahedron shaped figure.

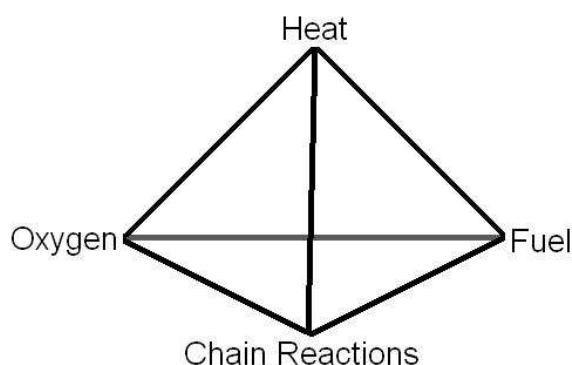


Figure 2. The fire tetrahedron (MAIIF Draft Guideline, 2011).

The tetrahedron shows every element has an interaction with the other elements (MAIIF, 2011).

3.1 The role of fuel and heat in a fire

Solid or liquid materials do not burn. In order for combustion to take place the materials need to be heated sufficiently to produce vapours. These vapours do have the potential to burn. Under laboratory conditions a set of important temperature points for materials have been derived:

Flashpoint: the lowest temperature in which a liquid or solid material produces enough vapour to burn.

Flamepoint: the lowest temperature in which the fuel produces enough vapour to sustain a continuous flame.

Ignition temperature: also referred to as auto ignition point, the temperature at which the vapour will ignite without a spark. If the source of the heat is an open flame or spark, it is referred to as piloted ignition.

Based on these temperature values a distinction between combustible and flammable materials can be made; a combustible material is capable of burning (generally in air under normal conditions in ambient temperature and pressure), whereas a flammable material is only capable of burning with a flame (MAIIF, 2011).

3.2 The role of the oxygen level in a fire

The concentration of oxygen is determinant for the continuation and type of fire. An atmospheric concentration of at least 15 to 16 percent is needed for continuous flaming combustion. The atmosphere normally contains approximately 20.8 percent of oxygen already. Without the oxygen level needed for flaming combustion, the fire is still able to smolder if the oxygen is higher than 8 percent. This so called smoldering is defined as the transformation of a compound into one or more other substances by heat alone (MAIFF, 2011). The other type of oxygen poor fire is pyrolysis. Pyrolysis is the combustion of materials due to a sufficient external source of heat enabling to cause the material to burn without a flame. The difference between smoldering and pyrolysis is that smoldering does not need an external source to supply enough heat for combustion, because the internal heat of the material itself suffices (Mulholland, 2008). Besides the atmosphere, certain chemicals are able to provide oxygen by acting as oxidizers supplying a direct source of oxygen or indirect source (in their combustion oxygen is formed) (MAIFF, 2011).

3.3 The role of chain reactions, mixing and proportioning in a fire

In order for a fire to continue mixing and proportioning (chain) reactions must be continuous, because the fuel vapours and the oxygen must be mixed in the correct proportion. Also the density of the fuel vapour is important for the fire continuance. The vapour needs to be heavier than air, because then it will sink to ground level making it possible for the fire to continue. If the vapour is lighter than dry air, the fuel will rise to relative calm atmosphere (MAIFF, 2011).

3.4 Fire transfer and stages in fire development

In a normal compartment a fire will develop through three predictable stages: incipient stage, free-burning stage and smoldering stage. It is important to know direct flame contact is not the only way for a fire to develop: a fire is also able to transfer via conduction, convection and radiation (MAIFF, 2011).

3.4.1 Fire transfer through conduction

Conduction is the transfer of heat via direct contact through a solid body. The ability of fire to transfer via conduction from one compartment to another is dependent on the solid body material: wood for example is a poor conductor, whereas metals are known to be good conductors (MAIFF, 2011).

3.4.2 Fire transfer through convection

Convection is the transfer of heat caused by changes in density in liquids and gases: the heat transfers through the motion of heated matter. It is the most common method for heat to transfer in a fire. Convected heat moves in predictable patterns contributing to the so called convection cycle. Heated air is lighter than cool air, therefore the heated air and smoke produced by the combustion will rise above the cool air. The cool air will take their place where it is also heated by the fire. Meanwhile the heated air and gases raised by the fire will cool off and drop down to be reheated again (MAIFF, 2011).

3.4.3 Fire transfer through radiation

Radiation is the transfer of heat by infrared radiation (heat waves) with no material or substances involved. The heat travels outward of the fire in the same manner as light, using all directions unless it is blocked. When the radiated heat contacts a body, the body could absorb, reflect or transmit the heat. If the body absorbs the heat, the temperature of the body will rise. Fire is able to extend

through radiation, because radiation is able to heat combustible substances in the fires pathway, causing them to produce vapours, and then ignite the vapours (MAIIF, 2011).

3.4.4 *Fire transfer through direct flame contact*

Fire transfer through direct flame contact is a combination of two basic methods of heat transfer. Hot gases from the flame rise and when contacting additional fuel, heat transfer through convection takes place. Meanwhile the radiant heat causes the additional fuel to produce vapours, which could be ignited by the flame (MAIIF, 2011).

3.4.5 *Incipient stage in fire development*

The incipient stage of a fire starts at the moment of ignition. At this moment the flames are localized. During the incipient stage the fire is regulated by the configuration, mass and geometry of the fuel. The oxygen level is still within normal range and normal temperatures are still present. Through convection a plume of hot fire gasses will rise, which draws additional oxygen into the bottom of the flame. If there is a solid fuel above the flame, both convection and direct flame contact will occur, causing an upward and outward fire spread resulting in a characteristic V-shape pattern on vertical surfaces (MAIIF, 2011).

3.4.6 *Free-burning stage in fire development*

During the free-burning stage the fire is intensifying and consuming more fuel. The flames spread upward and outward from the point of origin through convection, conduction and direct flame contact. The smoke and fire gasses are starting to accumulate at the upper level of the compartment and radiate heat downwards. The soot and gasses will continue to accumulate until one or more fuels reaches its ignition point. At this point rollover occurs: ignition of the upper layer of fuel gasses results in a fire extending across the compartment at his upper levels. Due to the rollover the overhead temperature the downward radiation increases, resulting in secondary fires. At this point the fire is still fuel regulated. If the temperature keeps increasing and reaches 593°C sufficient heat is generated for a simultaneous ignition of all fuels in the compartment, referred to as flashover. Flashover results in intense burning of the compartment and its contents. After flashover the fire is still fuel regulated, except if the fire stays in original compartment it will become oxygen regulated. The time a fire needs to develop from the incipient stage to flashover is dependent on the fuel package, compartment geometry, and ventilation (MAIIF, 2011).

3.4.7 *Smoldering stage*

The free-burning stage will consume the fuel. After the fuel is consumed and the fire is contained, the oxygen level will drop below 15 to 16 percent. At this point the fire is in the pyrolytic or smoldering stage. The fire now is oxygen regulated even if there is still unburned fuel (MAIIF, 2011). The difference between smoldering and pyrolysis is that smoldering is self-sustaining, whereas pyrolysis needs an external source of heat. Most materials can be pyrolyzed, but only few materials are able to smolder (Mulholland, 2008).

4 Formation of particles in smoke production

The properties of smoke are primarily determined by the particle concentration and size distribution. The combustion conditions under which smoke is produced (flaming, pyrolysis, or smoldering) affect the amount and character of the smoke. At the time it is not possible to predict smoke emission as a function of fuel chemistry and combustion conditions. However it is possible to give a description of smoke production and smoke properties as a function of flaming, pyrolysis, and smoldering conditions (Mulholland, 2008).

4.1 Particle formation in pyrolysis and smoldering combustion

During pyrolysis and smoldering fuel fragments rise at the fuel surface as a result of an elevated temperature, which is between 300°C and 600°C for pyrolysis, and for smoldering between 300°C and 800°C (Mulholland, 2008). Because the only difference between pyrolysis and smoldering is that pyrolysis requires an external heat source while smoldering is self-sustaining, it is assumed that smoke formation for smoldering is very similar to smoke formation in pyrolysis. Moreover only a few materials are able to smolder, while most of the materials can be pyrolyzed. During pyrolysis fuel fragments rise from the surface, but also a vapour emerges. This vapour possibly contains fuel monomer, partially oxidized products, and polymer chains. As the vapour rises, the low vapour pressure constituents are able to condense, forming smoke droplets appearing as light-colored smoke (Mulholland, 2008).

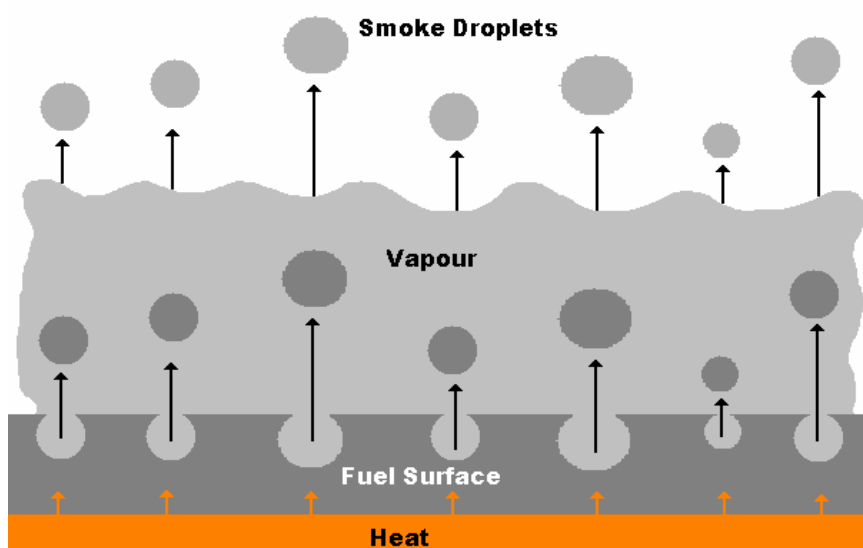


Figure 3. Formation of smoke droplets in pyrolysis or smoldering conditions. Due to heat, fuel fragments and vapour rise. Condensation of the vapour on the fuel fragments, causes the formation of smoke droplets appearing as light-colored smoke (Mulholland, 2008).

4.2 Particle formation in flaming combustion

The formation of smoke aerosols in flaming combustion is a more complex process. First fuel fragments pyrolyze from the surface. In the high temperature of the flame environment, these fragments react to form acetylene, benzene, and radical species including H, OH, and small hydrocarbon radicals. The one-ring benzene undergoes a number of reactions involving acetylene and the radical species, resulting in multiple-ring species termed as polycyclic hydrocarbons (PAHs). The PAHs continue to grow to ultimately form the smallest soot particles, which are in the order of a few nanometres (Kennedy, 1997). Subsequent particle growth takes place by surface addition of acetylene and particle-particle collisions (coagulation). Next the particle growth continues due to agglomeration of these primary particles. The agglomeration process takes place in the flame, but some primary particles are partially fused in the post-flame environment as well, because the agglomerates are held together by dispersion forces. As the smoke is leaving the flame environment, PAHs are able to condense on the surface of the soot particle. The amount of condensed organics is generally less than 20% for overventilated fires, whereas for underventilated fires the fraction can increase up to 50% and the agglomerates develop a more coagulated structure (Leonard et al, 1994).

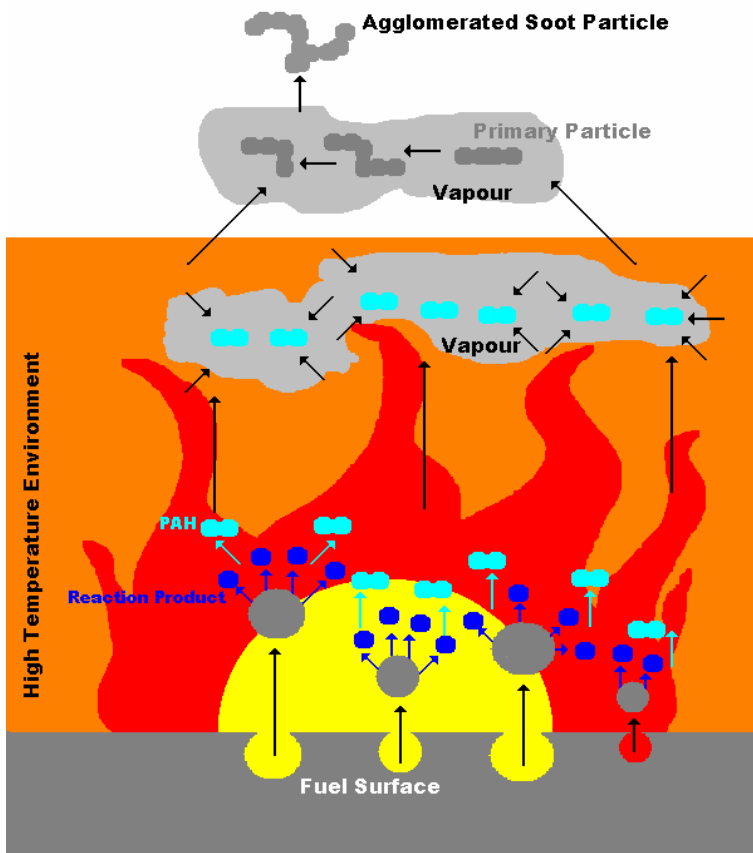


Figure 4. In flaming combustion fuel fragments pyrolyzes from the surfaces. The fragments react into products such as benzene, acetylene, H, OH and small hydrocarbon radicals. These products react into PAHs. The PAHs continue to grow. Subsequent particle takes place by coagulation and condensation, forming primary particles. Further coagulation and condensation of primary particles forms agglomerated soot particles (Butler & Mulholland, 2004).

4.3 Particle yield

Particle yield is defined as the percentage of the mass of a burning material which is converted into particles. If the air flow is less than what is required for complete combustion (underventilated fires), the soot yield usually increases. Tewarson found that smoke generation efficiency under ventilation controlled conditions increased up to 2.8 times for six materials (Tewarson et al, 1993). When predicting particle and soot concentration in smoke production it is important to determine whether the fire is flaming, pyrolyzing or smoldering, because smoke yield is generally larger in pyrolysis and smoldering (Mulholland, 2008). Also the particle fraction is lower in flaming smoke (Bankston et al, 1977; Bankston et al 1978). Moreover in pyrolyzing and smoldering conditions relative large amount of particles are found for materials that do not burn well. Well-burning materials e.g. wood tend to oxidize all available substances and thereby minimize the amount of particles in smoke (Hertzberg & Blomqvist, 2003).

4.4 Particle size distribution

Despite the large amount of particles which are generated in a fire relative few investigations have been made on particle size distribution and composition. The particle size is dependent on the material, temperature and fire conditions. Typical particle sizes of the spherical droplets from smoldering combustion are generally of the order of 1 μm , while those of irregular soot particles from flaming combustion are often larger, but much harder to determine dependent on the measuring technique and sampling position (Stec & Hull, 2010). Because of the complex shape of the agglomerated particles formed by a flame, there is a lack of an independent verification of the aerodynamic size distribution of particles formed in flaming combustion (Butler & Mulholland, 2004).

Despite the absence of an independent verification Butler and Mulholland performed data-fits for particle size distribution under flaming conditions in 2004. In these data-fits the particle size distributions are described as a function of the geometric average of the particle diameter (Butler & Mulholland, 2004). Mulholland performed the same type of data-fits in 2002 for pyrolysis or smoldering conditions. Both for flaming conditions and pyrolysis / smoldering the particle size distribution is a log-normal function of the geometric average of the particle diameter. However the geometric standard deviation in flaming conditions is determined by the number of particles in the i^{th} interval, whereas the geometric deviation in pyrolysis is determined by the total number of particles as well as the number of particles in the i^{th} interval (Butler & Mulholland, 2004; Mulholland 2008).

In flaming conditions the geometric average particle diameter size and geometric standard deviation is given by formulas 1 and 2:

$$\log d_{g(f)} = \frac{\sum n_i \log d_i}{\sum n_i}$$

Formula 1

$$\log \sigma_{g(f)} = \left[\frac{\sum n_i (\log d_g - \log d_i)^2}{\sum (n_i) - 1} \right]^{1/2}$$

Formula 2

$d_{g(f)}$ = geometric averaged particle diameter in flaming conditions

n_i = number of particles in i^{th} interval

d_i = particles sizes in i^{th} interval

$\sigma_{g(f)}$ = geometric standard deviation inflaming conditions

In pyrolysis or smoldering the geometric average particle diameter size and geometric standard deviation is given by:

$$\log d_{g(p)} = \sum_{i=1}^n \frac{N_i \log d_i}{N}$$

Formula 3

$$\log \sigma_{g(p)} = \left[\sum_{i=1}^n \frac{(\log d_i - \log d_{gn})^2 N_i}{N} \right]^{1/2}$$

Formula 4

$d_{g(p)}$ = geometric averaged particle diameter in pyrolyzing conditions

N_i = number of particles in i^{th} interval

N = total number of particles

d_i = particles diameters in the i^{th} interval

$\sigma_{g(p)}$ = geometric standard deviation in pyrolyzing conditions

The data-fits indicate that a geometric standard deviation could differ from approximately 2 to 16 (Butler & Mulholland, 2004; Mulholland, 2008).

5 Smoke plume dispersion trajectory

During a fire a rising smoke plume is released into the atmosphere. The dispersion trajectory of the smoke plume can be divided into two processes: plume rise and passive dispersion in horizontal and vertical direction, see figure 5.

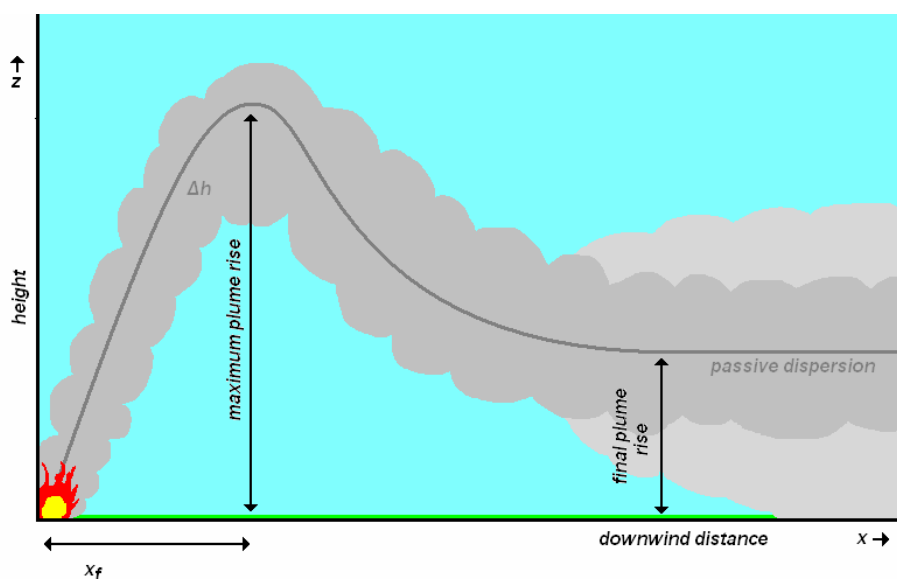


Figure 5. Cross-section of a major fire plume.

There is little data available on the actual smoke plume dispersion emitted by a fire, because in case of a fire there are often other priorities than data collection. Also an experiment with major fires is difficult to perform, because of the environmental impact and possible dangers of uncontrolled fires (Mennen et al, 2009). However there is a relative large amount of data available on controlled stack smoke emissions. It has been assumed that the basic equations for stack emissions also apply for smoke emissions by fires. The major difference between fire and stack emission, is that stack emissions are being controlled. The emitted smoke in stacks is defined as a mixture of gasses, and suspended particles. It is proposed that small particles behave gas-like, whereas larger particles are likely to deposit due to gravitational forces (Sijm et al, 2007).

In general materials released in the atmosphere rise because it contains upward momentum and/or the material is less dense (buoyant) compared to the surrounding air. The final height of the plume rise is determined by the mixing with the atmosphere. When vertical motion of the plume is of the same magnitude as the turbulent motion, it is assumed the plume is at its final height. However in case the atmosphere is steadily stratified the height at which the released material is in equilibrium with the density of the air is assumed to be the height of the final plume rise. After the plume has risen to its final height, dispersion is assumed to be passive (CPD, 2005).

5.1 Atmospheric stability

The atmospheric stability is a very important parameter for smoke plume dispersion, since it affects plume rise (Beychock, 2005), and the passive horizontal and vertical dispersion (Van de Meent & De Bruin, 2007). Atmospheric stability is a term applied qualitatively to the property of the atmosphere which governs the acceleration of the vertical motion of an air parcel. Unstable atmospheric conditions represent a decrease of potential temperature with height causing an acceleration of air parcels, because the turbulence increases. In neutral atmosphere the potential temperature is constant with the height, which means the acceleration is zero. In stable atmospheres the potential temperature increases with height meaning the turbulence is suppressed, which causes a deceleration of air parcels (Mohan & Siddiqui, 1998). This also explains why atmospheric stability during day time is different compared to night time. At day time the potential temperature near the earth's surface is higher due to sunlight reflection. This potential temperature decreases with the distance to the earth's surface, explaining why in general during day time the atmosphere is unstable. At night time there is no solar reflection, which eventually leads to stable atmospheric conditions.

There are seven main atmospheric stability classes designated as:

- A: highly unstable or convective
- B: moderately unstable
- C: slightly unstable
- D: neutral
- E: moderately stable
- F: extremely stable
- G: low wind night time stable conditions

Historically the stability classes A-F have been proposed by Pasquill and Gifford and further improved by Turner, and therefore known as the Pasquill-Gifford-Turner (PGT) stability classes (Turner, 1970). Later the seventh class G has been introduced for stable night time conditions.

The atmospheric classification proposed by Pasquill and Gifford is often used in consequence and risk analysis (Marx & Cornwell, 2009). In more thorough atmospheric modelling the stability is not classified, but parameterised by using the Monin-Obukhov length and the Richardson number. The flux of the Richardson number is the ratio between the production of kinetic energy by (heat-induced) buoyancy and the production of kinetic energy by mechanical turbulence velocity, see formula 5 (CPD, 2005):

$$R_f = \frac{K_T}{K_M} R_i$$

Formula 5

- R_f = Flux Richardson number
- K_T = Diffusivity by heat transfer
- K_M = Turbulent momentum diffusivity
- R_i = Richardson number gradient

Atmospheric buoyancy could also result in a loss of kinetic energy. This means the Richardson number flux can be negative. The Monin-Obukhov length is the height when the production of kinetic energy by buoyancy is equal to production of kinetic energy by turbulence velocity ($R_f = 1$) and could be derived as given in formula 6 and 7 (CPD, 2005):

$$L = z / R_f$$

$$L = \frac{-\rho C_p T_0 u_*^3}{\kappa g q_z}$$

Formula 6

Formula 7

- L = Monin-Obukhov length (m)
- z = atmospheric boundary layer height (m)
- R_f = Richardson number flux
- ρ = density ($\text{kg}\cdot\text{m}^{-3}$)
- C_p = heat capacity ($\text{W}\cdot\text{K}^{-1}\cdot\text{kg}^{-1}$)
- T_0 = absolute temperature ($^\circ\text{K}$)
- u_* = friction velocity ($\text{m}\cdot\text{s}^{-1}$)
- κ = Von Karman constant (0.4, dimensionless)
- g = gravitational acceleration ($\text{m}\cdot\text{s}^{-2}$)
- q_z = vertical mean turbulent heat flux ($\text{W}\cdot\text{m}^{-2}$)

Note that the Richardson number in formula 6 as well as the vertical mean turbulent heat flux in formula 7 could both be negative (night time) or positive (day time) meaning the Monin-Obukhov length could be negative or positive as well. This is determinant for the atmospheric stability (CPD, 2005):

$L > 0$	Stable	$q_z < 0$
$L < 0$	Unstable	$q_z > 0$
$L \approx \infty$	Neutral	$q_z = 0$

These relations between Monin-Obukhov length, atmospheric stability and vertical heat flux has been interpreted by Seinfeld & Pandis as shown in table 1.

Table 1. Interpretation of stability conditions corresponding with Monin-Obukhov lengths (Seinfeld & Pandis, 1998).

<i>Monin-Obukhov Length (L)</i>	<i>Interpretation</i>	<i>Stability Condition</i>
$-100\text{m} < L < 0\text{m}$	Small negative	Very Unstable
$-10^5 \text{ m} \leq L \leq -100 \text{ m}$	Large negative	Unstable
$ L > 10^5 \text{ m}$	Very large (positive or negative)	Neutral
$10\text{m} \leq L \leq 10^5\text{m}$	Large positive	Stable
$0\text{m} < L < 10 \text{ m}$	Small positive	Very Stable

5.2 Plume rise

Crucial for plume rise is a sufficient buoyancy factor ($F_b > 55$). Plumes with an insufficient buoyancy factor are considered to be cold jet plumes with a trajectory dominated by its initial velocity momentum, whereas plumes with a sufficient buoyancy factor are considered to be hot, buoyant plumes dominated by their buoyant momentum (Beychock, 2005). The buoyancy factor can be derived as a result from the heat of the emitted gas (or gas-like behaving particles) as shown in formulas 8 and 9 (Van Jaarsveld, 2004):

$$F_b = \frac{g}{\pi} V_f \left(1 - \frac{T}{T_s}\right)$$

Formula 8

$$F_b = 8.8Q_h$$

Formula 9

F_b = buoyancy factor ($m^4 \cdot s^{-3}$)

g = gravitational acceleration ($m \cdot s^{-2}$)

V_f = Volumetric flow rate ($m^3 \cdot s^{-1}$)

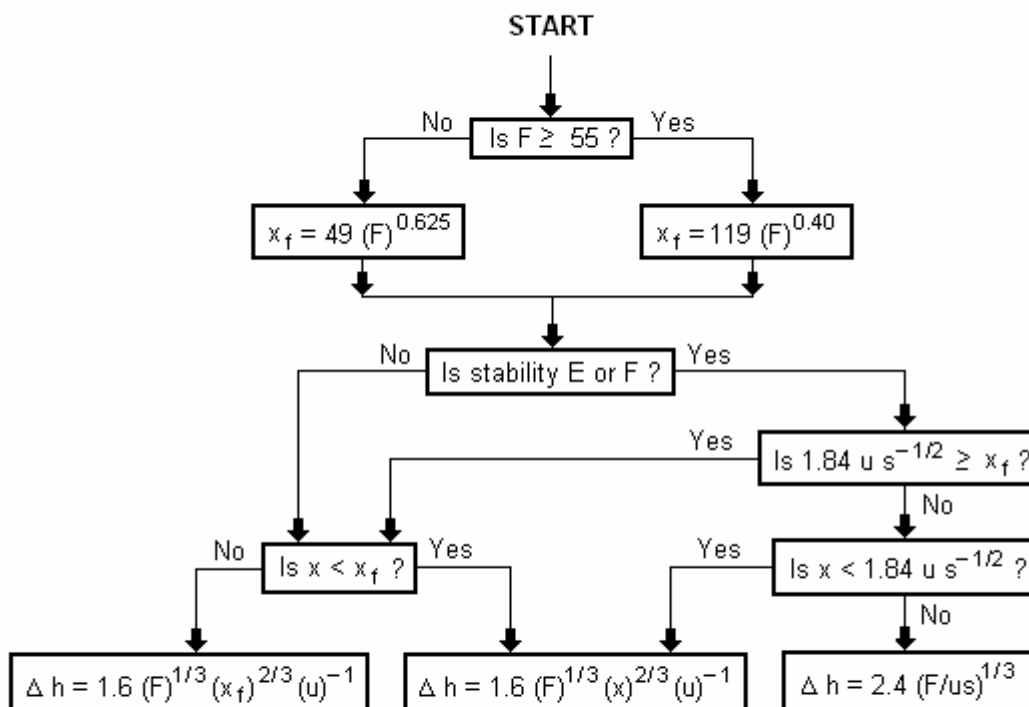
T = ambient temperature ($^{\circ}K$)

T_s = smoke temperature ($^{\circ}K$)

Q_h = heat output (MW)

Based on the atmospheric stability, the wind speed and the buoyancy factor the maximum plume rise height and the horizontal location (x_f) of the maximum plume rise can be derived by applying the Briggs Equations (Beychock, 2005). In 1969 Briggs performed a classical critical review on the entire plume rise literature in which he proposed a set of plume rise equations, which have since then become the widely known and widely used Briggs Equations (Briggs, 1969). Subsequently, Briggs modified his plume rise equations in 1971 and in 1972 (Briggs, 1971; Briggs 1972). A logic diagram for using the Briggs Equations proposed by Beychock in 2005 is presented below.

LOGIC DIAGRAM FOR BRIGGS' EQUATIONS TO CALCULATE THE RISE OF A BUOYANT PLUME



Δh = plume rise, in m
 F = buoyancy factor, in m^4/s^3
 x = downwind distance from plume source, in m
 x_f = downwind distance from plume source to point of maximum plume rise, in m
 u = windspeed at actual stack height, in m/s
 s = stability parameter, in s^{-2}

Figure 6. Logic diagram for Briggs' Equations to calculate the rise of a buoyant plume (Beychock, 2005).

5.3 Passive dispersion by the commonly used Gaussian Plume Model (GPM)

A commonly used air model for passive dispersion is the Gaussian Plume Model (GPM). The GPM is a Lagrangian model describing dispersion over short distances from the source (maximum 30km). Assuming that turbulence is a random process, it is expected that the mean concentration of material emitted from a point source will have a two-dimensional Gaussian distribution perpendicular to the mean wind direction. In its simplest form the GPM describes concentrations at a specified location, $C_{x,y,z}$ using the following equation:

$$C_{x,y,z} = \frac{Q}{2\pi u \sigma_y \sigma_z} \cdot \left[e^{-\left(\frac{y^2}{2\sigma_y^2}\right)} \right] \left\{ e^{-\left(\frac{(z-H)^2}{2\sigma_z^2}\right)} + e^{-\left(\frac{(z+H)^2}{2\sigma_z^2}\right)} \right\}$$

Formula 10: Gaussian Plume Model

$C_{x,y,z}$ = concentration at a certain x,y and z coordinate ($\text{kg}\cdot\text{m}^{-3}$)

Q = source strength ($\text{kg}\cdot\text{s}^{-1}$)

u = wind speed ($\text{m}\cdot\text{s}^{-1}$)

H = effective source height: (the sum of stack height and) plume rise (m)

σ_y = dispersion coefficient in horizontal direction (m)

σ_z = dispersion coefficient in vertical direction (m)

The horizontal σ_y and vertical σ_z dispersion coefficients are dependent on the travel distance and the atmospheric stability. Therefore expressions are developed by Gifford in order to correlate σ_y and σ_z with atmospheric variables based on the Pasquill stability classes [Gifford, 1961]. These correlations are commonly known as the Pasquill-Gifford curves. For use of the GPM formula the expressions are empirically determined as:

$$\sigma_z = R_z x^{r_z}$$

Formula 11

$$\sigma_y = R_y x^{r_y}$$

Formula 12

R_y , R_z , r_y and r_z are empirical parameters, which depend on the stability class and averaging time. The values of these parameters can be found in textbooks [Van de Meent & De Bruin, 2007]. In the national applied method for the calculation physical effects of chemicals released in the atmosphere (The Yellow Book) the empirical values in table 2 are used.

Table 2. Empirical values applied in the national method for calculation of chemicals released in the atmosphere (CPD, 2005).

Stability Class	R_z	r_z	R_y	r_y	
Very unstable	A	0.28	0.90	0.527	0.865
Unstable	B	0.23	0.85	0.371	0.866
Slightly unstable	C	0.22	0.80	0.209	0.897
Neutral	D	0.20	0.76	0.128	0.905
Stable	E	0.15	0.73	0.098	0.902
Very stable	F	0.12	0.67	0.065	0.902

5.4 Atmospheric boundary layer and mixing height

Another important parameter which has a significant role to play in atmospheric dispersion is boundary layer depth (Mohan & Siddiqui, 1998). Substances released into the atmospheric boundary layer (ABL) are gradually dispersed vertically through the action of turbulence. If there are no significant sinks, the emitted substances will gradually become completely mixed within this layer. The mixing height, which is defined as the depth of the ABL, determines the volume available for the dispersion of aerosols and gases (Campanelli et al, 2003). Empirically the mixing height can be defined as the "the height of the layer adjacent to the ground over which pollutants or any constituents emitted within this layer or entrained into it, become vertically dispersed by convection or mechanical turbulence within a time scale of about an hour" (Seibert et al, 1998). A low mixing height leads to high particle concentrations near the ground, while larger mixing height values result in lower concentrations near the surface. The top of the boundary layer acts as an inversion layer or a lid for upward streams carrying aerosol particles, so that relatively high and constant number and mass concentrations can be found within the ABL. In the free atmosphere above the ABL there is usually a lower aerosol concentration (Campanelli et al, 2003). Emission sources with high buoyancy factors (e.g. major fires) are able to (partially) penetrate through this inversion layer, whereas plumes emitted by low buoyancy factors are trapped below the inversion layer as shown in figure 7 and 8.

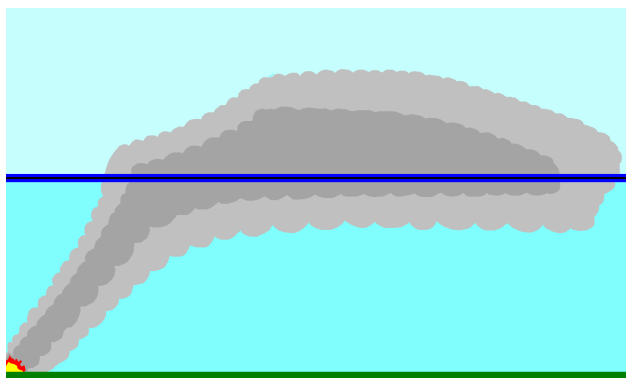


Figure 7. Plume with high buoyancy emission (partially) penetrating through inversion layer (Bluet et al, 2004).

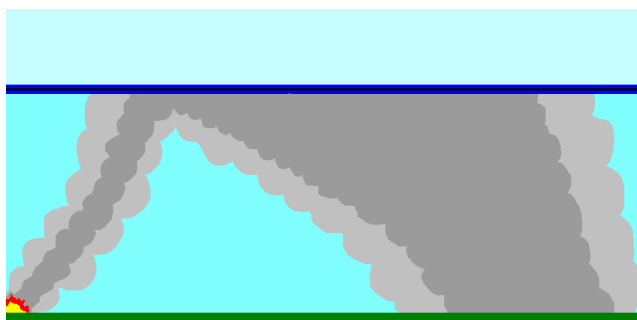


Figure 8. Plume with buoyancy emission trapped under inversion layer (Bluet et al, 2004)

Smoke plumes penetrating the inversion layer correspond with lower air concentrations at breathing level and lower deposition concentrations, because the concentrations of particles reaching the free atmosphere will be diluted into lower concentrations (Bluett et al, 2004).

6 Atmospheric deposition

Particles released in a fire will disperse through the air and deposit to the ground. In atmospheric chemistry it is customary to present deposition mechanisms as being composed of wet (precipitation-mediated) deposition and dry deposition mechanisms. Wet deposition is the sum of rain-out (precipitation processes inside a cloud) and wash-out (precipitation processes under a cloud). Dry deposition is defined as the sum of aerosol deposition and gas absorption (Sijm et al, 2007).

6.1 General dry deposition of materials

The dry deposition of materials in general should be regarded as the transport of a chemical passing through a series of resistances. The main resistances occur at the interface between air and surface. Here is transport of the material from the air to the surface, diffusion across the interface and transport from the interface to the solid surface. The deposition velocity (V_d) is dependent on the atmospheric turbulence, the chemical composition and the physical structure of the receiving surface and the depositing material (Sijm et al, 2007).

6.2 Dry deposition of particles

The dry deposition of a particle can be described as a function of its physical characteristics, of which size is the most important one. Small particles tend to behave like gases, whereas larger particles ($>2\mu\text{m}$) are efficiently removed by gravitational forces. For particles between 0.1 and 10 μm dry deposition occurs through inertial impaction which greatly depends on the air velocity and turbulence. Removal of a chemical through dry particle deposition is proportional to the concentration of the chemical in the particle and the deposition velocity of these particles. Large particles ($>10\mu\text{m}$) are deposited primarily by sedimentation and generally will be deposited close to the source. Because the lifetime of a particles in the air, greatly depends on their size, it is important to know the size of the particles as they leave the source (Sijm et al, 2007). A quantitative prediction of the amount of released particles and their size distribution cannot be made, only a few assumptions (see Chapter 4). The rate of the deposition of a substance bound to particles to the surface can be expressed according to formula 13:

$$Dep_{dry(particle)} = V_{d(particle)} \cdot Area_{surface} \cdot C_{air} \cdot FR_{particle}$$

Formula 13

$Dep_{dry(particle)}$ = dry deposition rate of particles ($\text{mol}\cdot\text{s}^{-1}$)

V_d = deposition velocity ($\text{m}\cdot\text{s}^{-1}$)

$Area_{surface}$ = area of the air-soil interface (m^2)

C_{air} = concentration of particles in the air ($\text{mol}\cdot\text{m}^{-3}$)

$FR_{particle}$ = fraction of substance associated with particle

Deposition velocities for particles are strongly related to the physical properties of the particles, of which the particle diameter is the most important. Very small particles ($<0.1\mu\text{m}$) deposit primarily through Brownian diffusion and large particles ($>2\mu\text{m}$) through gravitational settling. But also the properties of the surface area are important for the deposition velocity. Key factors of the surface are vegetation height, sizes of collecting elements, stickiness, wetness, and turbulent velocities above the surface area (Van Jaarsveld, 1995). A plot of the relationship between particle size and deposition velocity in neutral conditions accounting for Brownian diffusion, inertial impaction and gravitational acceleration is shown in figure 9.

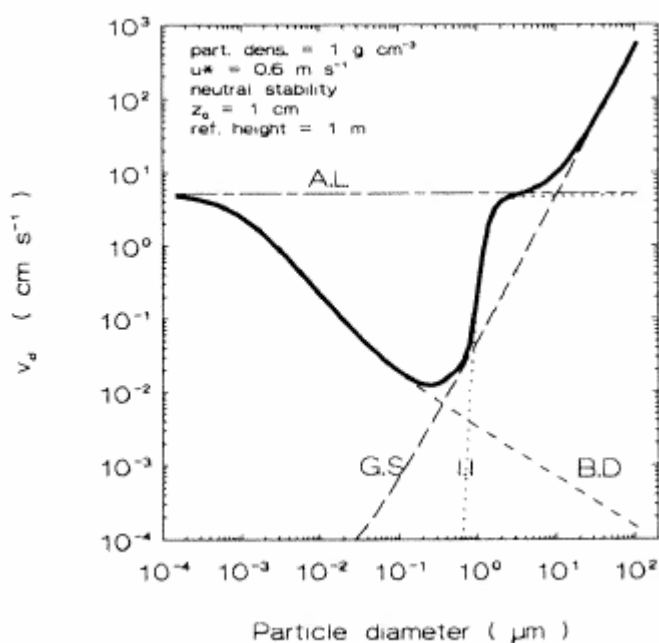


Figure 9. Deposition velocity as a function of particle size due to the processes aerodynamic limitation (A.L), gravitational settling (G.S) inertial impaction (I.I) or Brownian diffusion (B.D) (Van Jaarsveld, 1995).

6.3 General wet deposition of materials

Wet deposition includes two major processes: wash-out and rain-out. Wash-out is the absorption of gases and particles in the falling rain drops under the cloud. Rain-out is the scavenging of gases and particles in the cloud by the cloud droplets. Gases and particles taken up by the cloud will be removed from the droplets in the next rainfall (Sijm et al, 2007).

6.4 Wet deposition of particles

In general the removal rate by wet deposition can be described by a first order process with a scavenging coefficient (Λ), consisting of a gas and particle component. As a practical approach for estimating the scavenging coefficient of the particle $\Lambda_{particle}$ Mackay has suggested that during rainfall, each drop sweeps through a volume of air about 200,000 times its own volume taking down all particles in it (Mackay, 1991). Wet deposition of particle bound substances can be described as in the following equations (Sijm et al, 2007):

$$Dep_{wet(particle)} = \Lambda_{particle} \cdot Area_{surface} \cdot h \cdot C_{air}$$

Formula 14

$$\Lambda_{particle} = \frac{J}{h} \cdot 2 \cdot 10^5 \cdot FR_{particle}$$

Formula 15

$Dep_{wet(particle)}$ = wet deposition rate of particles ($mol \cdot s^{-1}$)

$\Lambda_{particle}$ = particle scavenging coefficient (s^{-1})

$Area_{surface}$ = area of the air-soil interface (m^2)

h = height of the mixed layer (m)

C_{air} = concentration of particles in the air ($mol \cdot m^{-3}$)

J = rain intensity ($m \cdot s^{-1}$)

$FR_{particle}$ = fraction of substance associated with particle

7 Toxicity of fire released airborne particles and particle bound substances

In order to understand the toxicity concentrations of airborne particles and the deposited substances bound to the particles, it must be clear what those hazardous substances are. It is also important to understand their toxicological mechanisms and what fire conditions affect their emission concentration.

7.1 Measurements of particulate matter and particle bound substances at fire sites in the Netherlands

The Environmental Accident Service (MOD) of the RIVM has published an overview report of analysed air and deposition samples taken in the surroundings of more than 50 fires in The Netherlands from 1997 till 2007. This overview report of the MOD includes particulate matter and particle bound components. Based on the measurements made, the MOD has presented an overview of released particulate matter and particle bound substance for different types of fires and burning materials (Mennen & Van Belle, 2007). See table 3:

Table 3. Overview of released particulate matter and particle bound substance measured for different types of fires and burning materials (Mennen & Van Belle, 2007).

Type of fire or material	Particulate Matter	PAHs and bifenyles	Dioxines	Miscellaneuous organic components	Lead	Zinc	Copper	Miscellaneuous elements
Synthetics C-H	+++	+++	-	-	-	-	-	-
PVC and PVC-likes	+++	+++	++	Chlorate PAHs, PCBs	-	-	-	-
Synthetics O	+++	+++	-	Fenoles, alcohols, furanes, carbonic acids, esthers	-	-	-	-
Synthetics N	+++	+++	-	Nitro-PAHs	-	-	-	-
Synthetics S	+++	+++	-	Sulphur containing PAHs	-	-	-	-
Additives in synthetics	(++)	(++)	(+)	Phtalates, organobromic- and organophosphorus bindings	(+)	(+)	(+)	Ba, Cd, Cr, Co, Ni, Sb, Ti, Ca, As, Se, Hg, P
Rubbers and car tyres	++	+++	-	Sulphur-PAHs, organosulphur- and organobromic bindings	-	++	-	Br
Oil and oil-derived fuels	+++	++	-	Organosulphur bindings, sulphur-PAHs	-	-	-	-
PCB oils and transformers	++	+++	+++	Chlorate PAHs	+	+	++	Ni, V
Paint, solvents, pesticides and other chemicals	++	+++	(+++)	Multiple bindings	(+)	(+)	(+)	Fe, Al, Cr, Sb, Cd, Sn, Ba
Wood, paper, carton	+	++	(+)	Aldehydes, furanes, fenoles	-	-	-	-
Garbage	(+++)	(+++)	(++)	Multiple bindings	(+)	(+)	(+)	Multiple bindings
Cacao	++	+	-	Nitrilles, carbonic acids, lipic acid esters	-	-	-	-
Buildings	++	++	(++)	Multiple bindings	++	++	++	Ba, Ca, Cr, Ni, Sb, Sn, Ti

The table shows that PAHs, dioxins and elements in the heavy metals category (*Pb, Cu, Zn, Cd, Cr, Ti, Ni, V, Fe, Co, Hg, Sn, Sb, Al*) are the most common found particle bound components. Particulate matter itself is released in every type of fire or material.

7.2 Toxicity of airborne particles

Particles in the air are associated with various health effects (EEA, 2009). Therefore the particle concentrations measured in the air are also regarded as hazardous. Originated from combustion airborne particles can be compromised as a complex mixture of carbon, metals, and polyaromatics (Madl et al, 2010). The fire conditions affecting the emission of particles are already discussed in Chapter 4. Their toxicological mechanisms are explained below.

7.2.1 Toxicity of airborne particles

The relevant exposure route for particulate matter is through inhalation. There are a number of factors that influence whether a particle is toxic or relatively inert:

- Respirability
- Patterns for pulmonary deposition
- Clearance and retention
- Solubility
- Surface reactivity

Where and how many particles are deposited in the respiratory tract is determined by the physical mechanisms of the particles and by the biology of the subject inhaling the particles. The five most significant mechanisms of particle respiratory tract deposition are:

- Sedimentation and impaction: a function of the inertial aerodynamic size characteristics.
- Diffusion: a function of the diffusional properties of the particle.
- Interception: occurs when one of the edges of the particles touches the surface of the respiratory tract (a major determinant of fibre deposition).
- Electrostatic precipitation: a function of electric charged particle attraction to the respiratory tract surface. In general electrostatic precipitation can be neglected, since particles gradually lose their electric charge in the environment.

(Madl et al, 2010)

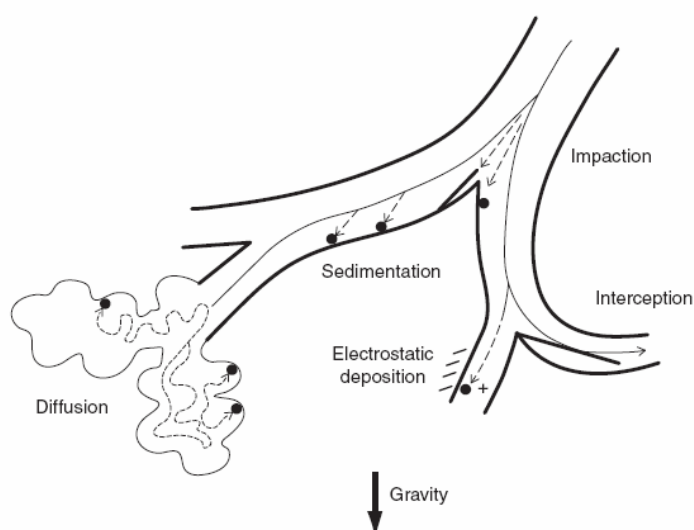


Figure 10. Primary mechanisms of deposition of inhaled particles in the respiratory tract (Madl et al, 2010).

Size is an important characteristic of the particle in determining the respiratory tract deposition. Larger particles ($>2\text{-}3\mu\text{m}$) act primarily by inertial mechanisms and preferentially deposit in the upper respiratory tract, whereas smaller particles ($<100\text{nm}$) act by diffusion and will deposit in the nasopharyngeal, tracheobronchial, alveolar and gas exchange regions of the lungs. Once particles are deposited within the respiratory tract the mechanism by which they are cleared not only depends on the location in the lungs, but also on the size and chemistry of the particle (Madl et al, 2010). Solid particles are removed from the lungs through a variety of mechanisms:

- Sneezing, coughing, and removing mucus from the nasopharyngeal region
- Direct or macrophage-mediated transport along the mucociliary escalator and subsequent elimination by the gastrointestinal tract
- Direct or macrophage-mediated transport across the bronchiolar or alveolar epithelium and subsequent clearance by the systemic circulation or interstitial lymphatics
- Physicochemical processes, including dissolution, leaching, and physical breakdown of particles.

(Madl et al, 2010)

Comparisons of transport patterns of different size particles suggest that nanosized particles are retained in the lungs to a greater extent than particles in the fine-size range ($0.1\text{-}2.5\mu\text{m}$). Fine-size particles are more retrieved by macrophages (Ferin, 1991; Oberdorster et al, 2005). Also nanosized particles lack the rapid phase clearance typically observed for larger-sized particles (Roth et al, 1993). Additionally research suggests that nanosized particles clear slower because they are more readily taken up by epithelial cells and therefore less likely to be cleared by macrophage (Kreyling et al, 2004). Because the transport patterns differ per particle size, the probability of particles depositing in a certain respiratory tract region is determined by the particle size, see figure 11.

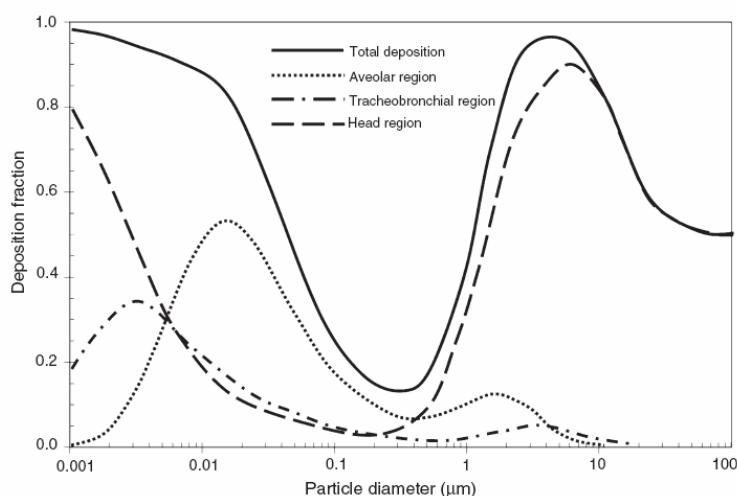


Figure 11. Particle deposition probability in different regions of the respiratory tract for different particle diameter sizes (ICRP, 1994).

The presence of particulate matter in the respiratory tract leads to a number of adverse biological effects:

- Inflammation
- Cytotoxicity
- Oxidative stress
- Fibrosis
- Cellular and organ homeostasis
- Immunological cellular and humoral responses

(Madl et al, 2010)

These biological effects could act as a starting point for a variety of adverse health effects e.g. cardiovascular disease, respiratory disease and cancer.

7.3 Polycyclic aromatic hydrocarbons (PAHs)

Polycyclic aromatic hydrocarbons (PAHs) are organic compounds consisting of two or more aromatic rings.

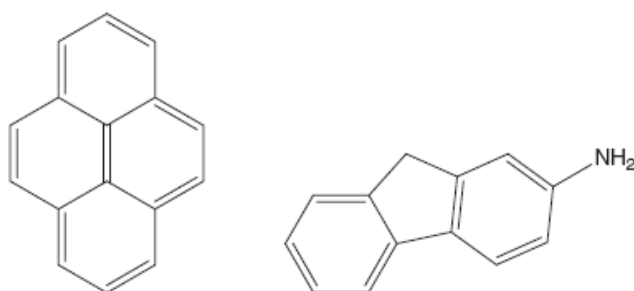


Figure 12. General chemical structure of PAHs.

They are a product of the incomplete combustion of organic or carbon containing material. PAHs are lipophilic, meaning they mix more easily in oil than water. Because of these properties, PAHs in the environment are found primarily in soil, sediment and oily substances, as opposed to water or air. Furthermore in combustion processes PAHs are able to grow into particles via coagulation and addition of gas-molecules (Richter & Howard, 2000).

7.3.1 Toxicity of PAHs

PAHs are produced by the incomplete combustion of organic material. The compounds are largely absorbed into smoke particles. Dermal contact, ingestion, and inhalation are possible exposure routes. When absorbed via the gastrointestinal tract PAHs are metabolically transformed to more reactive forms. A number of PAHs have a carcinogenic and mutagenic potential. Some PAHs are more toxic than others, but their mechanism of toxicity often relies on adduct formation with macro-molecules following biotransformation (Gad & Gad, 2005). Benzo(a)pyrene is often used as an indicator PAH species, because it has the most carcinogenic potential (Mennen & Van Belle, 2007). The exposure limit for benzo(a)pyrene proposed by the Occupational Safety and Health Administration is 0.2 mg m^{-3} .

7.3.2 *Fire conditions affecting PAH emissions*

In any fuel combustion PAH formation and emission mechanisms can be classified in two processes: pyrolysis and pyrosynthesis. During pyrolysis organic compounds are cracked by the heat into small and unstable fragments, which are mainly highly reactive free radicals with a very short lifetime. In the pyrosynthesis process the unstable fragments recombine with each other into stable PAH molecules (Mastral & Callén, 2000). For the formation of PAHs, combustions conditions are more important than fuel properties (Mastral & Callén, 2000). Ventilation is an important factor influencing the PAH formation in a combustion process: an increase of excess air leads to great decrease PAH formation. Temperature is also of influence. The highest emission rates of PAHs are found in temperatures between 750 to 850°C. Above 850°C the emission of PAH is controlled by ventilation (Mastral & Callén, 2000). However there are also some evidences suggesting that very small amounts of PAHs can also be formed during pyrolysis with a temperature range of 350-600°C (Garcia-Perez, 2008).

7.4 **Dioxins**

Dioxin is a substance category for compounds consisting of two benzene rings interconnected by two oxygen atoms.

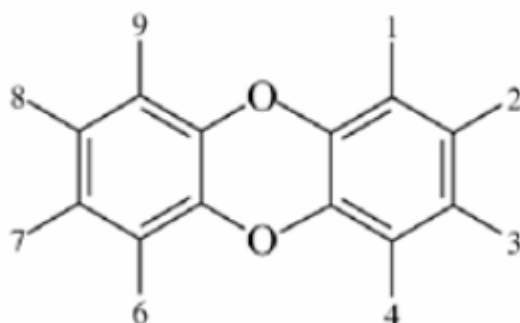


Figure 13. General chemical structure of dioxins.

Dioxins with chlorine atoms are of particular environmental concern, because the water solubility of the dioxin decreases and the solubility in organic solvents and fats increase with increasing chlorine content. Furthermore dioxins are characterized by extreme low water solubility, and have a tendency for being strongly adsorbed on surfaces of particulate matter (Al-Alawi, 2008).

7.4.1 *Toxicity of dioxins*

Most high-level exposures to dioxins are results from accidental releases or explosions in chemical plants or storage facilities for dioxin-containing chemicals. Dioxins are persistent in the environment and have a high bioaccumulation potential. Exposure may occur via the soil, air (especially when dioxins occur as combustion products), or water.

Dioxins are highly lipid soluble and poor substrates for metabolic enzymes enabling them to exhibit high liver concentrations and accumulate in fatty tissue. The excretion of dioxins is therefore extremely slow: the elimination half-life in humans is approximately 10 years. The toxic effects of dioxins could be caused by interaction with the Ah-receptor intracellular protein, ultimately leading to alterations in genetic expression.

Short term toxic effects of dioxins include headache, fatigue, irritation of the gastrointestinal and respiratory tracts, dehydration and skin irritation. A generally accepted minimum dose for humans is $0.1\mu\text{g}\cdot\text{kg}^{-1}$ (Young, 2005).

7.4.2 *Fire conditions affecting dioxin emissions*

The factors affecting the emission of dioxins during a fire are the properties of the burning material and the combustion conditions. If the burning material contains organic material with organochlorine compounds or even inorganic chlorides, dioxins can be generated in the fire. Important materials affecting the amount of released dioxins in a combustion process are:

- Dioxins that is already present in the burning material
- Dioxin precursors in the burning material
- Chlorine and chlorine containing products.

Important combustion conditions are:

- Combustion temperature
- Residence time of the dioxin molecule in the fire
- Oxygen availability

Together these conditions determine the combustion efficiency, which is discussed in paragraph 7.4.2.1 -7.4.2.4. If the fire has high combustion efficiency the formed dioxins are being destroyed or their formation is being prevented (Al-Alawi, 2008).

7.4.2.1 Presence of dioxins in the fuel

There is a widespread commercial use of dioxin containing products such as wood conservatives and pesticides. During inefficient or poorly controlled combustion of these products, it is very likely the dioxins are released to the atmosphere (Al-Alawi, 2008).

7.4.2.2 Presence of dioxin precursors in the fuel

Incomplete combustion of organic compounds could lead to the formation of organic fragments able to act as organic precursors of a dioxin molecule. Studies performed on dioxin precursors have centred on three major classes with a widespread use, see table 4.

Table 4. Major dioxin precursor classes and their widespread use (Al-Alawi, 2008).

<i>Class</i>	<i>Use</i>
Chlorinated phenols	Wood preserves, herbicide, and sap stain products
Chlorinated benzenes	Solvents, dyes, pharmaceuticals, and rubber production
PCBs	Dielectric fluids in transformers and capacitors, hydraulic fluids, plasticizers, and dyes

These organic precursors are potential dioxin forming compounds, because they are able to adsorb on the surface of fly ash in the post-combustion zone, and the following a complex series of chemical reactions catalyzed by metals lead to the formation of dioxins or other chlorinated organics (Al-Alawi, 2008).

7.4.2.3 Presence of chlorine in the fuel

Generally chlorine must be present for the formation of dioxins and general trends indicate that increased chlorine concentrations in the burning material improve the possibility of dioxin emission. Laboratory studies have indicated a correlation between chlorine input and dioxin emissions. However no significant correlation has been shown in field tests. Therefore the exact role of chlorine is still uncertain (Al-Alawi, 2008)

7.4.2.4 Combustion conditions

High combustion efficiency results in a low amount of released dioxin. In order to obtain high combustion efficiency the temperature should be high, the oxygen supply should be high, and the residence time of a dioxin molecule in the fire should be long. Experiments suggest that temperatures between 500-800°C promote the formation of dioxins, whereas temperatures greater than 900°C destroy the dioxins. Also the higher the combustion temperature, the less residence time is required for the dioxin molecule to be destroyed (Al-Alawi, 2008). Since increase of combustion efficiency leads to a decrease of dioxin release, it can be expected that during fire dioxin is mostly released in the incipient and smoldering stage when the combustion efficiency is low.

7.5 Heavy metals and airborne metals

There are no general principles that govern the toxicity for all heavy metals, only a few generalizations on metals are possible. Oxidation state and solubility of metals are critical factors in toxic reactions. Metals can react with enzymes, cell membranes, and specific cell components. These reactions can inhibit or stimulate the actions of these substances and components.

For the general population the primary exposure to metals is via ingestion of food or drinking water. Acute toxicity from metals shows similar effect patterns, namely nausea and vomiting. A few metals are carcinogenic to humans; the vast majority is not (Gad, 2005).

In general inhalation is a secondary exposure route for metals. However in case of airborne metals inhalation becomes more important. Metals emitted from combustion processes are usually particles with size in the fine mode. They show respiratory tract deposition characteristics and clearing mechanisms similar to general particulate matter. However close to the emission source electric precipitation becomes a more important mechanism, since the metal particles have not lost their electric charge yet (Graham et al, 2010). Health effects associated with airborne metals are:

- Respiratory pathophysiological effects: e.g. bronchitis, fibrosis, pneumonia, inflammation
 - Immunological respiratory defence effects: e.g. allergic responses, asthma, bronchitis
 - Carcinogenesis
- (Graham et al, 2010)

8 Literature research conclusions

The literature study showed that soil contamination due to particles released in a fire is dependent on a complex entity of many factors of influence. In the schematic overview in figure 14 a contributing factor is either regarded as a parameter or a process. Parameters can influence each other directly or indirectly in a process. A process cannot be expressed in units and is defined as an interaction of (input) parameters resulting into new (output) parameters. A parameter is defined as a variable determining the state of a process or system and can be expressed with units. Based on the review information in Chapter 3 to 7 a flow chart has been constructed considering all contributing parameters and processes. See figure 14. Table 5 appoints all the parameters in the flow chart and their corresponding scientific units. The review performed on all contributing parameters and processes is based on literature in different scientific areas. Therefore the flow chart only summarizes the performed review on a qualitative level.

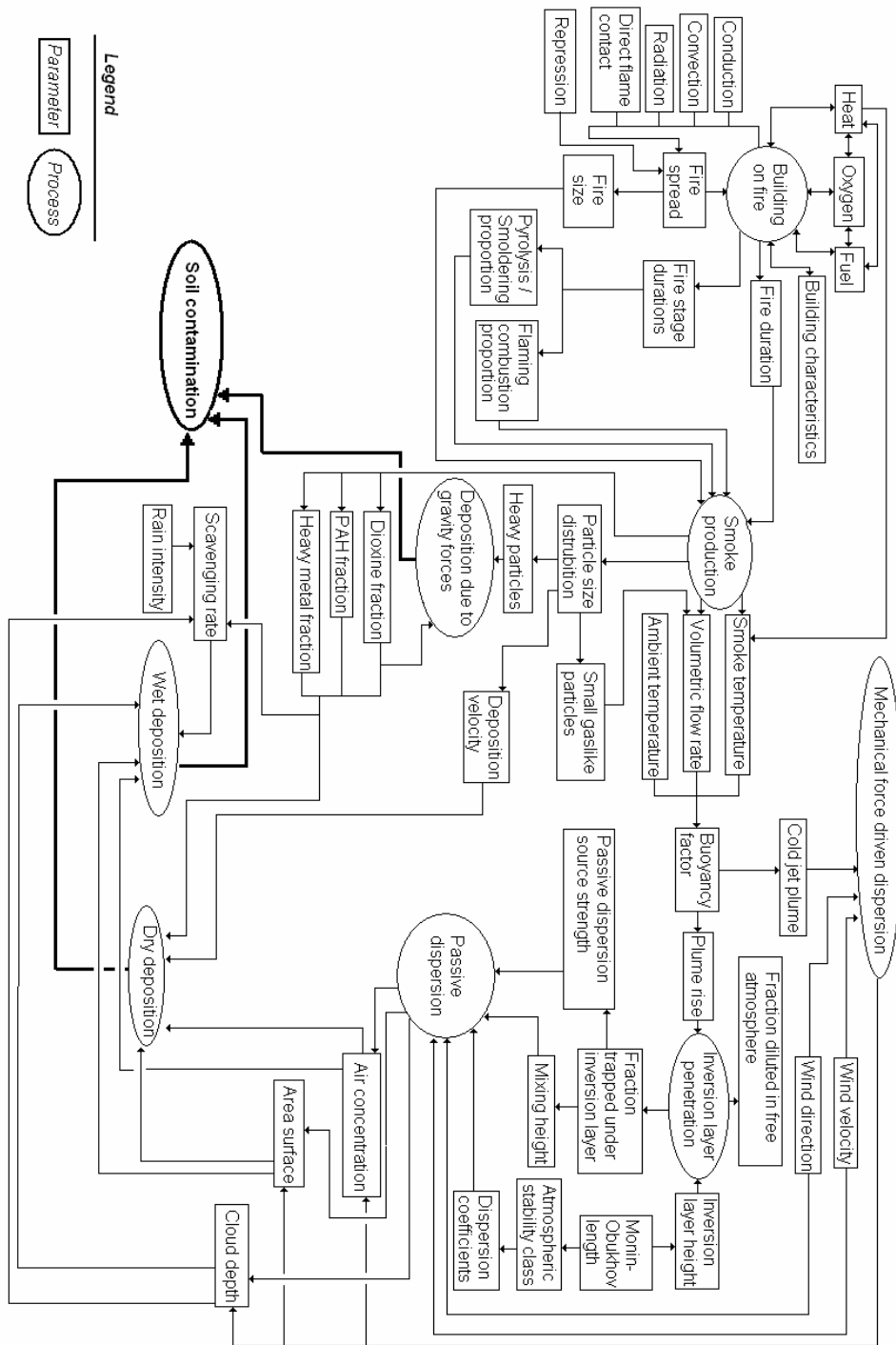


Figure 14. Flow chart of all contributing parameters and processes in the dispersion and deposition of particles released in a fire.

Table 5. Flow chart parameters and parameter units

<i>Parameter</i>	<i>Units</i>
Heat	MW
Oxygen	% in air
Fuel	kg material
Building characteristics	length: m height: m width: m
Fire spread	$m^2 \cdot s^{-1}$
Fire size	m^2
Fire duration	hours
Fire stage duration	hours
Pyrolysis / smoldering proportion	%.hours
Flaming combustion proportion	%.hours
Smoke temperature	$^{\circ}K$
Volumetric flow rate	$m^3 \cdot s^{-1}$
Ambient temperature	$^{\circ}K$
Plume rise	m
Cold jet plume	$m_{(x,y,z)}$
Buoyancy factor	$m^4 \cdot s^{-3}$
Particle size distribution	d_{gm} : μm σ_{gm} : dimensionless
Heavy particles	%
Small gas-like particles	%
Deposition velocity	$m \cdot s^{-1}$
Dioxin fraction	%
PAH fraction	%
Heavy metal fraction	%
Wind velocity	$m \cdot s^{-1}$
Fraction diluted into free atmosphere	%
Fraction trapped under inversion layer	%
Mixing height	m
Passive dispersion source strength	$kg \cdot s^{-1}$
Inversion layer height	m
Monin-Obukhov length	m
Atmospheric stability class	A,B,C,D,E,F
Dispersion coefficient	m
Air concentration	$mol \cdot m^{-3}$ ppm $mg \cdot m^{-3}$
Area surface	m^2
Cloud depth	m
Scavenging rate	s^{-1}
Rain intensity	$mm \cdot s^{-1}$
Norm values	$g \cdot m^{-2}$
Distance to the fire	m
Deposition Concentrations	$g \cdot m^{-2}$

9 CEVs' Current method in predicting the dispersion and deposition of particles released in a fire

For the prediction of the dispersion and deposition of particles released in a fire the CEV uses which is based on the basic principle of environmental modeling:

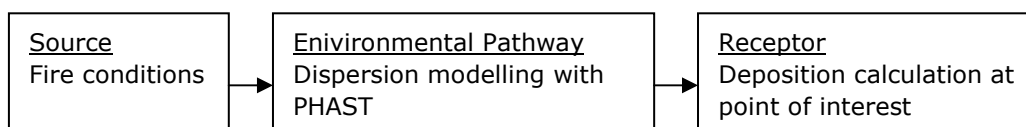


Figure 15. Interpretation of basic principle of environmental models applied in the method CEV uses for the estimation of the deposition of particles released in a fire.

9.1 Fire conditions

From a legal point of view two types of fire conditions are considered: 'PGS-15 fires' and 'miscellaneous fires'. PGS-15 fires are fires in warehouses that are constructed and operated conform to the directive in the 15th part of the Publication series for Hazardous Substances published by the former Ministry of Public Housing, Spatial Order en Environmental Management (VROM): so called PGS-15 warehouses.

9.1.1 PGS-15 fires

The PGS-15 directive describes the regulation for storing hazardous compounds on an acceptable safety level for humans and environment. All PGS-15 warehouses meet the same safety standards in fire prevention (InfoMil, 2007). This makes it possible to use assumptions which should be valid for all fire scenarios in a PGS-15 warehouse. According to the safety regulation the walls in a PGS-15 warehouse should be fire-resistant for at least 60 minutes and the roof construction for 30 minutes. In risk calculations it is assumed that the roof will collapse after 30 minutes and plume rise will occur. Before the roof collapses it is assumed the fire is still in its incipient stage and heat is being absorbed into the indoor environment resulting in relative cold smoke and combustion gasses. After the roof has collapsed the fire is assumed to be in its free-burning stage: the smoke and combustion gasses are barely being cooled down and are rising to great heights. Therefore at residential height hazardous concentrations are only expected before plume rise in the incipient fire stage. In principle no calculations are performed in case of visually observed plume rise (BOT-mi, 2010).

9.1.2 Miscellaneous fires

For miscellaneous fires the fire conditions must be determined for each fire separately. However the used approach in determining the fire conditions is the same. The potential impact is predicted based on the emission factors and the source term (source term is defined as the amount of released material, dimensions of the area, thermodynamic state of the substance, and the outflow velocity) (BOT-mi, 2010).

9.2 Deriving PHAST input data

For both PGS-15 fires and miscellaneous fires the modelling of the dispersion of the released particles is performed by PHAST. PHAST is a software package for consequence modelling of accidental releases of toxic or flammable chemicals to the atmosphere and is published by DNV Software, UK (Witlox, 2010). The model has no option for calculating dispersion and deposition for gas-like behaving particles release scenarios. Therefore in the method the dispersion of gas-like behaving particles is approached as dispersion of a neutral gas. In the CEV-method nitrogen is used as exemplary substance for the prediction of dispersion. The post-expansion data of nitrogen are the starting point (source term) of the subsequent dispersion modelling. In the dispersion modelling a wide range of scenarios can be made considering momentum, time-dependency, buoyancy, thermodynamic behaviour, ground effects, effects of jet, heavy-gas, passive dispersion, building wakes and ambient conditions (Witlox, 2010).

In order to calculate the desired PHAST output for the supposed release of particles, the model needs the following input:

Source emission data:

- Release rate ($\text{kg}\cdot\text{s}^{-1}$)
- Discharge rate ($\text{m}\cdot\text{s}^{-1}$)
- Pre-dilution air rate (kg air / kg nitrogen)
- Final release temperature ($^{\circ}\text{K}$)
- Release time (s)

Environmental data:

- Weather stability class (A-F)
- Wind speed
- Wind direction
- Building characteristics: height, width and length

9.2.1 Source emission input data

In the CEV-method nitrogen is used as a substitute for gas-like behaving particles. In order to determine the proper release rate for the substituting nitrogen the amount of released particles must be converted into a representing amount of released nitrogen. For this conversion the molecular weight of the particles and nitrogen is needed. See formula 14.

$$Q = N_{RP} \cdot (M_N / M_{RP})$$

Formula 14

Q = Release rate ($\text{kg}\cdot\text{s}^{-1}$)

N_{RP} = Amount of released particles ($\text{kg}\cdot\text{s}^{-1}$)

M_N = Molecular weight of nitrogen (g)

M_{RP} = Molecular weight of released particles (g)

If for example $20 \text{ kg}\cdot\text{s}^{-1}$ of nickel ($M=58.7$) is released in the form of particles the discharge rate would be:

$$Q = 20 \cdot (28/58.7) = 9.54 \text{ kg}\cdot\text{s}^{-1}$$

The CEV recognizes a major uncertainty in estimating the amount of released particles (N_{RP}) and the amount of hazardous substances bound to these particles, because there is little information available: only an assumed burning rate (fuel mass burning per second) and emission factors for a few materials (an emission factor is the mass proportion of burned fuel which is converted into an emission product) (BOT-mi, 2010). The burning rate is assumed to be $0.025 \text{ kg.m}^{-2}.\text{s}^{-1}$, whereas emission factors are dependent on the burned fuel and the emission product, see table 6. The emission factor values applied in the CEV-method are derived from RIVM Report 609021051/2007 (Mennen & Van Belle, 2007).

Table 6. The limited information available on release rate: Emission of factors for particles, PAHs en dioxins for a few fuel materials (Mennen & Van Belle; BOT-mi, 2010).

Fuel	Emission products					
	Particles		PAHs		Dioxins	
	Emission factor (g/kg fuel)	Release rate/m ² (g.m ⁻² .s ⁻¹)*1	Emission factor (g/kg fuel)	Release rate/m ² (g.m ⁻² .s ⁻¹)*1	Emission factor (g/kg fuel)	Release rate/m ² (g.m ⁻² .s ⁻¹)*1
Rubber	5-120	0.125-3.0	1-3	0.025-0.075	0.5-3	0.0125-0.075
Oil	40-130	1-3.25	~0.1	0.025	-	-
Wood	2-8	0.05-0.2	0.02-0.3	0.0005-0.0075	0.2-0.8	0.005-0.02
Shredder garbage of car wrecks	17-24	0.425-0.6	0.05-1	0.00125-0.025	-	-
Electronical devices	10-100	0.25-2.5	1-5	0.025-0.125	1.10 ⁻⁶ -2.10 ⁻⁵	0.25.10 ⁻⁶ -5.10 ⁻⁵

*1. Derived by multiplying the emission factor with the assumed burning rate of $0.025 \text{ kg.m}^{-2}.\text{s}^{-1}$

The release rate can be determined by multiplying the emission factor with burning rate and fire surface. In case of a miscellaneous fire little is known about the fires' source conditions. However in case of a PGS-15 fire some assumptions can be made. It is assumed only hazardous concentrations are present before plume rise and in the incipient stage. The release time is therefore assumed to be 1800s, because after half an hour the roof will collapse, plume rise will occur and no hazardous concentrations will be at residential height anymore. During this period only relative cold smoke and combustion gasses are released which are assumed to have a temperature of about 50°C and a discharge rate of $1\text{m}.\text{s}^{-1}$. For miscellaneous fires it is chosen not to deviate from these assumptions, unless there is an urgent reason to do so. For both PGS-15 fires and miscellaneous fires the influence of 'pre-dilution air rates' is assumed to be irrelevant, because past experiences with this parameter in the CEV-method have shown its influence is very small (BOT-mi, 2010). The default setting for pre-dilution air rate is therefore zero, unless there are reasons to believe there are large amounts of initial air mixture (BOT-mi, 2010).

9.2.2 *Building dimensions input data*

Building dimensions are important for the dispersion of the released substance, because the building surfaces perpendicular to the wind direction creates a building wake where the plume is able to dilute. In PHAST the effects of this building wake can be simulated by choosing the "Roof/Lee" option, which results in a different dispersion trajectory of the released substance with lower concentrations.

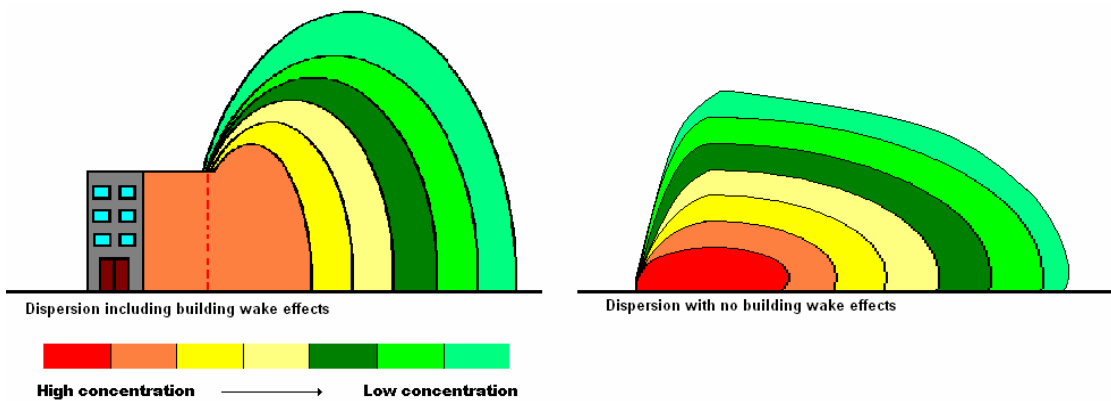


Figure 16: An illustration of the difference between cold jet plume dispersions with and without building wake effects derived from PHAST sideview graphs.

The broader and higher the building is, the more the substance is able to dilute. The length of the building does not influence the building wake size when it is parallel to the wind direction. Higher buildings also have another effect on the plume content. The plume is released at a higher point, causing a higher plume depth. The concentrations within the plume are lower because of the building wake dilution, but the large plume depth enlarges the height of the plume column and thus enlarges the plume column content. In case the released substance is heavier than air (which is the case for nitrogen, the exemplary substance the CEV-method prescribes) concentrations close to the ground will also be higher.

In general if the fire is indoor and little is known about the dimensions of the building the following assumptions are made (BOT-mi, 2010):

Table 7. Building dimensions applied in PGS-15 directive (BOT-mi, 2010).

<i>Building</i>	<i>Height</i>	<i>Length</i>	<i>Width</i>
Average warehouse	6m	17.3m	17.3m
Large warehouse	8m	30m	30m
Maximum sized warehouse	-	50m	50m

9.2.3 Atmospheric stability and wind input data

IN PHAST the weather conditions can be specified by selecting an atmospheric stability class and a wind speed. Wind speed is not independent from atmospheric stability. In order to choose a realistic wind speed, the value must be inside a range of possible wind speeds for a certain atmospheric stability class:

Table 8. Wind speed range per atmospheric stability class (BOT-mi, 2010)

<i>Atmospheric stability class</i>	<i>Wind speed range</i>
A	0 – 3 m.s ⁻¹
B	2 - 5 m.s ⁻¹
C	2- 6 m.s ⁻¹
D (daytime)	0- 6 m.s ⁻¹ or > 6 m.s ⁻¹
D (night time)	0-6 m.s ⁻¹
E	2-5 m.s ⁻¹
F	0-3 m.s ⁻¹

Wind direction is not relevant for the calculation of the plume, but only for the presenting calculated concentrations on the wind axes on a map.

9.3 Deriving deposition formula variable values from PHAST output

The CEV-method determines both dry and wet deposition fluxes. In order to estimate dry deposition PHAST output on the air concentration of particles at 1 m height (C_{air}) is needed. For wet deposition PHAST output on the column content of the entire plume above a certain point ($C_{plume} \times h$) is needed. The values for column content and air concentration at 1 m height are indirectly obtained from a sideview graph of the plume. Figure 17 is an example of a PHAST sideview graph:

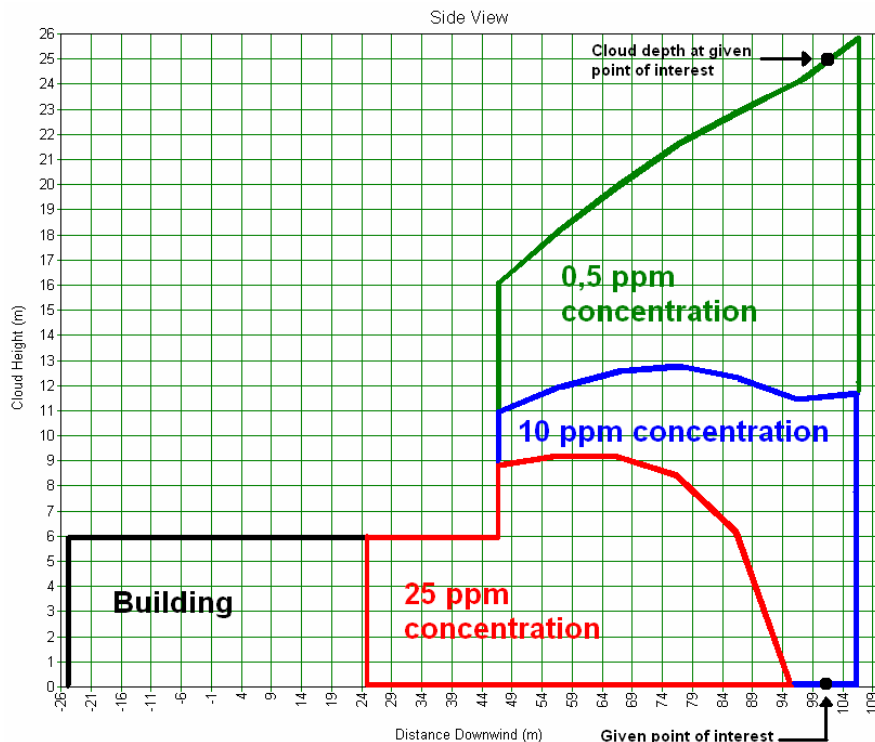


Figure 17: Example of a PHAST sideview graph. The dispersion of exemplary substance nitrogen is displayed in different concentration layers (in this example 25 ppm, 10 ppm and 0.5 ppm).

The concentration layers given in figure 17 are not necessarily the most representative or accurate presentations of the model outcome. In PHAST the concentration layer values are chosen personally. In order to find the most representative values one must try a range of different concentrations and then interpret personally what values are most representative. In order to use the found representative concentration values for the calculation of dry deposition fluxes the ppm-values must be converted into $\text{mg}\cdot\text{m}^{-3}$ values.

The average concentration within the total column (C_{plume}) has been derived by determining the 'cloud height' of each concentration profile in the PHAST sideview graph. For example in figure 17 PHAST was ordered to model concentration profiles for 25, 10 and 0.5 ppm. The 'cloud heights' for these concentration profiles at the given point of interest are:

Table 9. 'Cloud height' corresponding with concentration profiles in figure 17.

<i>Concentration</i>	<i>'Cloud height' at given point of interest</i>
25 ppm	0 m
10 ppm	12 m
0.5 ppm	13 m

C_{plume} is derived as the average of the concentrations in the entire column. In the example this would be:

$$C_{\text{plume}} = \frac{(25 \text{ ppm} \times 0 \text{ m}) + (10 \text{ ppm} \times 12 \text{ m}) + (0.5 \text{ ppm} \times 13 \text{ m})}{0 \text{ m} + 12 \text{ m} + 13 \text{ m}} = \frac{126.5 \text{ ppm} \cdot \text{m}}{25 \text{ m}} = 5.06 \text{ ppm}$$

Cloud depth 'h' is determined as the total 'cloud height' at the given point of interest in the sideview graph. In exemplary figure 17 this would be 25m.

9.4 Calculation of particle deposition

Using the CEV-method the estimation of deposition is based on a formula for wet and dry deposition. The variables in these formulas are assumptions, outcomes of PHAST model calculations, and observations or measurements. See formulas 15 and 16, and table 10.

$$F_{dry} = C_{air} \cdot V_d \cdot t$$

Formula 15

$$F_{wet} = C_{plume} \cdot h \cdot (J / J_0) \cdot \Lambda \cdot t$$

Formula 16

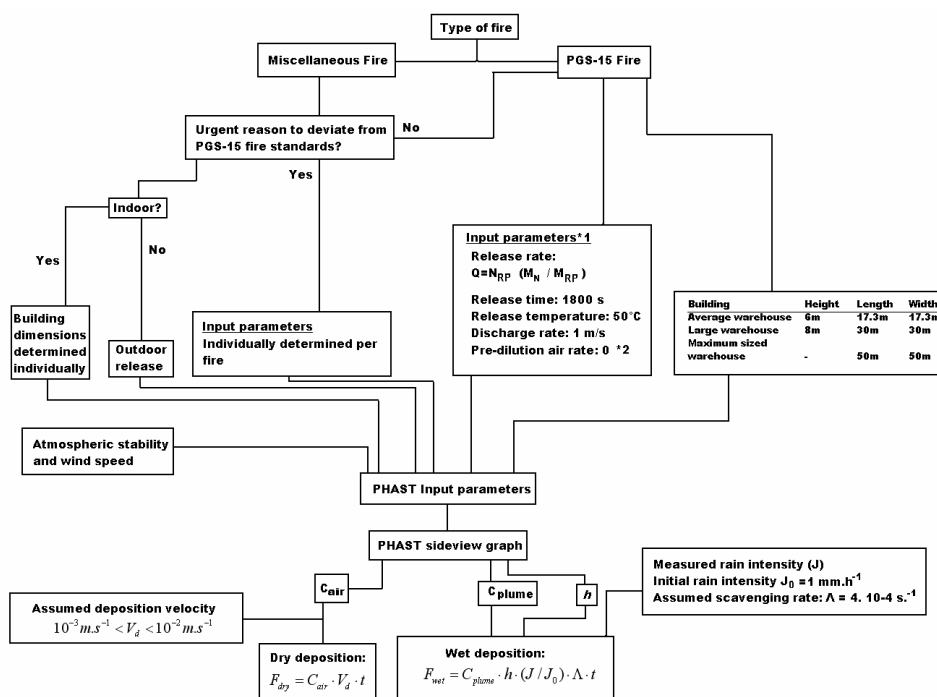
Table 10. Deposition variables used in the CEV-method.

	<i>Variable/ outcome</i>	<i>Description</i>	<i>Assumption / PHAST output</i>	<i>Value and / or unit</i>
Dry deposition	F_{dry}	Dry deposition flux	-	mg.m^{-2}
	C_{air}	Air concentration of particles at given location	PHAST output	mg.m^{-3}
	V_d	Deposition velocity	Assumption	0.01 m.s^{-1}
	T	Release time	Observed / Measured	s
Wet deposition	F_{wet}	Wet deposition flux	-	mg.m^{-2}
	C_{plume}	The average concentration of the column of the cloud above a given location	PHAST output	mg.m^{-3}
	H	Plume depth, height of the column of the cloud at given location	PHAST output	m
	J	Rain intensity	Observed / Measured	mm.h^{-1}
	Λ	Scavenging rate	Assumption	$4 \cdot 10^{-4} \text{ s}^{-1}$
	J_0	Rain intensity corresponding with the scavenging rate	Assumption (corresponding with Λ)	1 mm.h^{-1}

With formula 15 and 16 it is possible to apply a PHAST sideview graph for estimations for dry and wet deposition flux at any downwind point of interest.

9.5 Flow chart of CEV-method

The CEV-method can be summarized as a decision tree determining PHAST input parameter values. Based on the resulting PHAST sideview graph the wet and dry deposition flux is calculated using assumptions for deposition velocity (dry deposition) and scavenging rate (wet deposition). See figure 18.



*1: PGS-15 warehouse has fire-resistant walls for 60 minutes and roof construction should last for 30 minutes. Roof collapse is assumed to occur at 30 minutes. After roof collapse it is assumed there will be plume rise. In case of plume rise no hazardous concentrations. Only hazardous concentrations in the 'cold jet plume' before roof collapse.

*2 Unless there is reason to assume large amounts of pre-mixed air.

Figure 18. Flow chart of the CEV-method in predicting dispersion and deposition of particle released in fire.

9.6 Additional remarks by the CEV

“The CEV-method serves the possibility for estimating the order of magnitude of the particle deposition. The estimation of deposition fluxes based on a PHAST sideview graph is considered to be a rule of thumb and its results to be global. Moreover the deposition of particles is not considered to be an acute danger, but it has to be estimated for the sake of food protection. Any reported prediction value should be stated to be highly uncertain and public health measures should be based on measurements.” (BOT-mj, 2010)

10 Critical review on the CEV-method

10.1 Scientific background on deposition variable assumptions

For the estimation of dry and wet deposition the CEV-method uses assumptions. For dry deposition it is assumed that the 'deposition velocity' is between 10^{-3} $\text{m}\cdot\text{s}^{-1}$ and 10^{-2} $\text{m}\cdot\text{s}^{-1}$ and for wet deposition it is assumed that a 'scavenging rate' of 10^{-4} s^{-1} corresponds with a 'rain intensity' of 1 $\text{mm}\cdot\text{h}^{-1}$ (see paragraph 9.4). The scientific background of these assumptions is not directly presented in the instruction documents of the CEV-method. Therefore CEV-employees have been asked to give references to the literature they have used to underpin their assumptions. Paragraph 10.1.1 describes the scientific background of the assumed values for 'deposition velocity' and paragraph 10.1.2 describes the scientific background on the assumed value for 'scavenging rate'.

10.1.1 Deposition velocity, dry deposition

In order to investigate the background of the assumption of the dry deposition velocity a CEV employee has given a reference to the document 'NRPB-R182', a document produced by the National Radiation Protection Board (NRPB) of Great Brittan (NRPB, 1986). The prescribed values of 10^{-3} $\text{m}\cdot\text{s}^{-1}$ and 10^{-2} $\text{m}\cdot\text{s}^{-1}$ are regarded as rule of thumb and are based on the "expert judgment" of the NRPB on radio nuclides bound to particles from 1 -10 μm (NRPB, 1983). These recommendations are based on results of an earlier review on dry deposition velocity as a function of particle size performed by Slinn in 1978. The review performed by Slinn resulted in figure 19, where deposition velocity is described as a function of particle size.

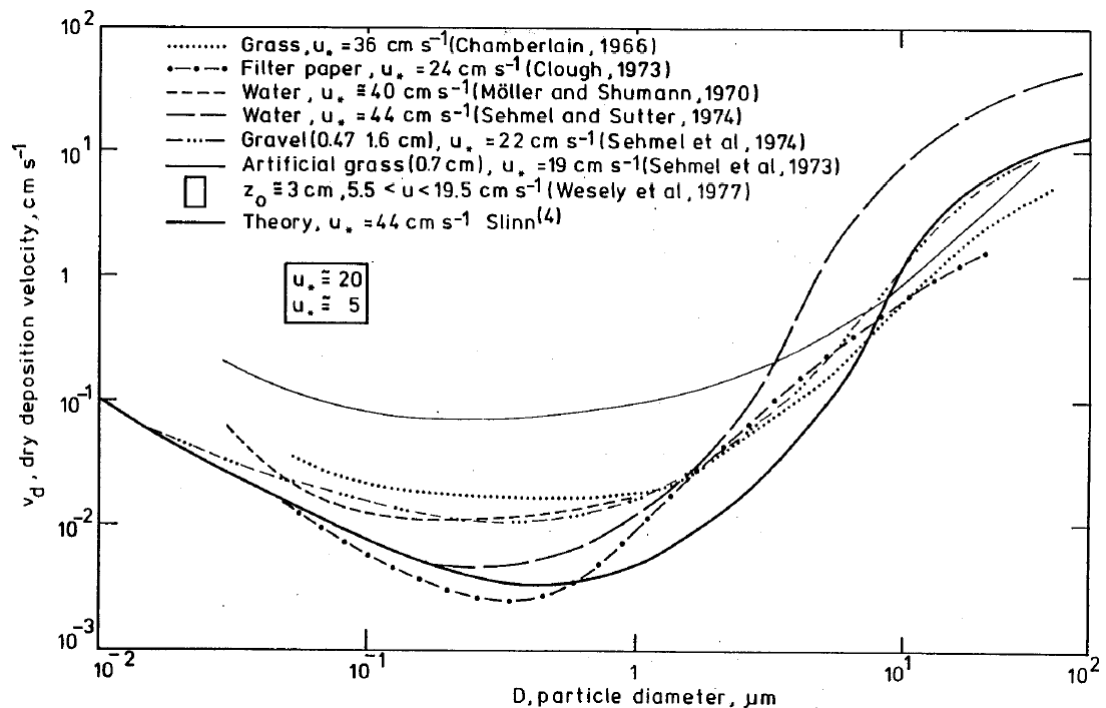


Figure 19. Deposition velocity as a function of particle size: origin of the assumed deposition velocity values (Slinn, 1978).

Based on figure 19 the NRPB has determined upper and lower limits.

Table 11. Upper and lower limits for deposition velocity as a function of particle size as determined by the NRPB (NRPB, 1983).

<i>Particle size</i>	<i>Deposition velocity (m.s⁻¹)</i>	
	<i>Lower limit</i>	<i>Upper limit</i>
1µm	10 ⁻⁴	10 ⁻³
10µm	10 ⁻²	3.10 ⁻²

In 1986 the NRPB has recommended to use the upper limits. The limits proposed by the NRPB are developed for worst case scenarios of nuclear disasters. The CEV however is focussed on dry deposition as a consequence of a large fire, which explains the chosen order of magnitudes for dry deposition velocity values.

Table 12. Interpretation by the CEV of the upper and lower limits for deposition velocity.

<i>Particle size</i>	<i>Dry deposition velocity (order of magnitude)</i>
1 µm	10 ⁻³ m.s ⁻¹
10 µm	10 ⁻² m.s ⁻¹

10.1.2 Scavenging rate, wet deposition

A scavenging rate of $4 \cdot 10^{-4} \text{ s}^{-1}$ for a rain intensity of $1 \text{ mm} \cdot \text{h}^{-1}$ is based on the legally determined Publication Series Hazardous Substances 2 (PGS-2): 'Methods for the calculation of physical effects', also referred to as the 'Yellow Book'. In the Yellow Book it can be found that for aerosols a scavenging rate is 'typically $4 \cdot 10^{-4} \text{ s}^{-1}$ for a precipitation of 1 mm per hour' (CPD, 2005). The typical value has been found by Bakkum in 1993, by determining a numeric algorithm for dry deposition and wash-out of emissions in the atmosphere (Bakkum, 1993). Alas the reference to this work was not available, because there was too little time left to request this relative old reference at its publisher TNO.

10.2 Parameters that are not (directly) included in the CEV-method

Not every parameter mentioned in the literature study is (directly) included in the CEV-method. This is the case for a number of source term parameters (parameters related to the 'building on fire'-process or characteristics of the emitted smoke) and some air dispersion parameters.

The source term parameters that are not (directly) included are:

- Heat (is indirectly included via the final release temperature)
- Oxygen supply
- Fuel (is indirectly included via emission factors and burning rate)
- Fire spread, via conduction, convection, radiation, or direct flame contact
- Repression
- Fire duration
- Fire stage duration
- Pyrolysis / smoldering proportion
- Flaming combustion proportion
- Dioxin fraction (is indirectly included via emission factors and burning rate)
- PAH fraction (is indirectly included via emission factors and burning rate)
- Heavy metal fraction
- Size distribution of particles formed in a fire

Air dispersion parameters that are not (directly) included are:

- Deposition velocity due to particle size distribution (is indirectly included by assuming deposition velocity is between 10^{-3} m.s^{-1} and 10^{-2} m.s^{-1})
- Plume rise (is indirectly included via the final release temperature)
- Inversion layer height

10.3 Indicative verification

Verification proves a model or calculation method solves the mathematical equations correctly. The model PHAST itself has already been verified by DNV Software (Witlox, 2010). However the calculation of wet and dry deposition based on PHAST output (sideview graph) has not been verified yet. Therefore an indicative verification has been performed using the principle that a multiplication of a release rate at the source will lead to the same multiplication at the endpoint.

The function of release rate on deposition concentration should be linear, because if all the other conditions stay the same a multiplication of the source strength must lead to the same multiplication at the endpoint, in this case the deposition concentration.

The verification has been performed for both wet and dry deposition. In case of wet deposition the release rate has been marked out against 'average cloud concentration multiplied by cloud depth ($C_{\text{cloud}} \times h$)', because these are the PHAST output parameters used in the calculation method for wet deposition. The other parameters in the wet deposition formula are regarded as constants. In the verification of the prediction of dry deposition the release rate has been marked out against air concentration at 1m height (C_{air}) and the other parameters in the dry deposition formula being regarded as constants. A range of release rates from 0,05 to 0,75 $\text{kg}\cdot\text{s}^{-1}$ has been inserted in step sizes of 0,05. The miscellaneous PHAST input parameters such as building size and atmospheric stability are the same in every step size and are given in table 14.

The released substance that is modelled in the verification method is nitrogen, because the CEV uses nitrogen as an exemplary substance. In figure 20 each step size in release rate has been plotted against the derived average cloud concentration multiplied by cloud depth. In figure 21 release rate has been plotted against cloud concentration at a height of 1 m. The downwind distance in figure 20 and 21 is 100m to the source.

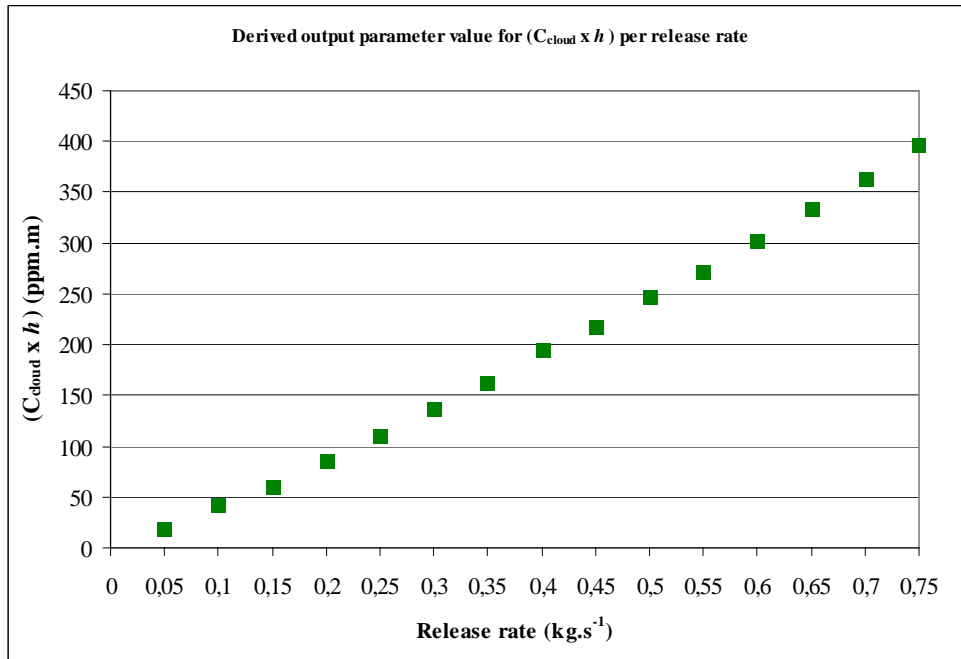


Figure 20. Average cloud concentration multiplied by cloud depth as a function of release rate modelled with PHAST.

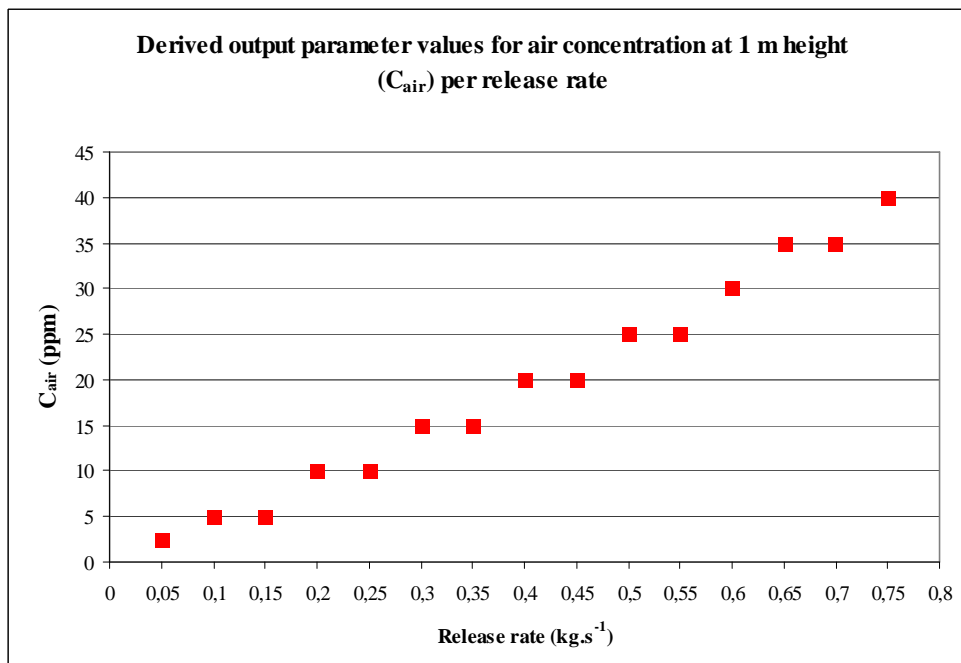


Figure 21. Air concentration at 1m height as a function of release rate modelled with PHAST.

Figure 20 shows a linear function between release rate and cloud depth multiplied by the cloud concentration seems to be linear indeed. Air concentration at 1 m height also seems to be linear to the release rate, as can be seen in figure 21. As far as the verification can indicate the CEV-method is not mathematically incorrect.

11 Sensitivity analyses: used models and methods

The description and the critical review of the CEV-method shows there are uncertainties in predicting dispersion and deposition of particles. The description of the method has shown that the inserted values for PHAST input parameters are often based on assumptions or limited information. In order to investigate what these input uncertainties mean for the resulting deposition flux, sensitivity analyses have been performed on the most important input parameters used in the method. A sensitivity analysis shows the influence of a parameter on the model outcome. In this study this influence is considered to be narrowing, broadening or linear. The sensitivity analyses have been performed by inserting a range of different input values for one parameter and determine the difference in the output values. If the difference in output is greater than the difference in input the parameter is considered to be sensitive and to have a broadening function. If the difference in input is approximately the same as the difference in the output the sensitivity of the parameter is considered to be neutral and its influence is linear. If the difference in input is larger than the difference in output, the parameter is considered to be insensitive and its influence narrowing, see table 13.

Table 13. Influences of the sensitivity of a parameter

<i>Sensitivity</i>	<i>Influence</i>
Sensitive	Broadening: a difference in input leads to a greater difference in output
Neutral	Linear: a difference in input leads to the same difference in output
Insensitive	Narrowing: a difference in input leads to a smaller difference in output

The critical review on the CEV-method has shown that the air dispersion parameters 'particle size distribution', and 'plume rise' (that are in scientific literature considered to be relevant) are not included in the CEV-method or included in an indirect way. This may result in uncertainty on the model outcome. The influence of these parameters however cannot be modelled with PHAST. Therefore for the sensitivity analyses of these parameters another air dispersion model has been selected: The Operational Priority Substance model-Short Term version (OPS-ST) developed by the RIVM.

11.1 Model selection for parameters particle size distribution, plume rise and inversion layer height: OPS- Short Term

The sensitivity analyses for the air dispersion parameters 'particle size distribution', and 'plume rise' have been performed with OPS-ST. OPS-ST has been selected for this task, because it is the most suitable air dispersion model made available to this study. The available models were: STACKs, NPK Puff, OPS- Long Term, and OPS-ST. These models have been assessed on suitability based on the 5 criteria described in the guideline for atmospheric model selection proposed by Van de Meent and De Bruin (Van de Meent & Bruin, 2007):

1. Spatial scale: Air concentration and deposition measurements show the required spatial scale should at least have a grid with 100m accuracy, because within this range particle concentrations may vary considerably (Mennen & Van Belle, 2007).
2. Temporal scale: A fire normally lasts a number of hours. The temporal scale therefore should at least show hourly averaged concentrations.
3. Components: The components regarded in this study are particles. The model therefore must be able to predict particle dispersion and deposition.
4. Computer facilities: The model must be able to run on a personal computer.
5. Required accuracy: The outcomes must be accurate enough for a sensitivity analysis.

The OPS-ST model meets the 5 criteria mentioned above. Also OPS-ST is able to process the parameters 'particle size distribution', 'inversion layer height', and 'plume rise' (Van Jaarsveld, 2004). Therefore the OPS-ST model has been selected for the performing the sensitivity analyses for these parameters.

11.2 Sensitivity analyses with PHAST

The sensitivity of the parameters that are considered to be important in the CEV-method are analysed with the PHAST model. These parameters are:

- Weather stability class (A-F)
- Building dimensions: height, width and length
- Release rate ($\text{kg}\cdot\text{s}^{-1}$)
- Pre-dilution air rate
- Final release temperature

Paragraph 9.3 describes there is no straightforward method in choosing representative values for the concentration layers in the PHAST sideview graphs. This means the sensitivity analysis results are partially based on a personal interpretation of 'representative concentration layer values'. Therefore the sensitivity analyses are based on at least 10 different concentration layers. The stepsize differences between the chosen concentration values for these layers are also never larger than 50%.

11.2.1 Default input values

When performing a sensitivity analysis for a certain parameter, the values for the other parameters mentioned above are set as default values. Table 14 shows these default values:

Table 14. Default input values for major input parameters in PHAST

<i>Input Parameter</i>	<i>Default value</i>
Building dimension	6m x 50m x 50m
Release rate	0,16 $\text{kg}\cdot\text{s}^{-1}$
Final release temperature	50°C
Pre-dilution air rate	0 $\text{kg}\cdot\text{s}^{-1}$
Weather stability class	D
Wind speed	6 $\text{m}\cdot\text{s}^{-1}$

The chosen default values in table 14 are based on the CEV-method which is described in Chapter 9. The default values for parameters 'final release temperature', 'pre-dilution air rate' and 'building dimensions' are based on the values derived from the PGS-15 directive as described in paragraph 9.2.1 and 9.2.2. The weather stability class is chosen to be D, because it represents neutral conditions. The wind speed is chosen to be 6 $\text{m}\cdot\text{s}^{-1}$ because this is a speed representative for the chosen stability class D.

The CEV-method does not describe values for the parameter 'release rate' in a straight-forward way. It is assumed that the few fuel materials and their particle emission factors given in table 6 are not representative for a building on fire. Therefore it is chosen not to perform a sensitivity analysis for the release of particles. Instead an indicatory sensitivity analysis has been performed for the release of nitrogen dioxide during a fire, because the estimation for release rate values of nitrogen dioxide during is described in the CEV-method in a straight-forward approach (BOT-mi, 2010). The values for the release rate of nitrogen dioxide used in the CEV-method are given in table 15.

Table 15. Release rate values of nitrogen dioxide as a function of fire size and nitrogen supply (BOT-mi, 2010).

Fire size	Nitrogen supply* ¹	Release rate NO ₂ * ² (kg.s ⁻¹)
300 m ²	1,5%	0,037
300 m ²	5%	0,123
600 m ² * ³	3,75%* ³	0,160* ³
900 m ²	1,5%	0,111
900 m ²	5%	0,369

*1 Relative amount of nitrogen holding products stored in the warehouse.

*2 The released substance in the sensitivity analysis is not NO₂, but N.

*3 Averaged value

The substance that is modelled however is not nitrogen dioxide (NO₂) but nitrogen (N) and the default value for the release rate of nitrogen is chosen to be 0.16 kg.s⁻¹ (Q= 0.16 kg.s⁻¹, see paragraph 9.2.1), because this is the average of the release rate values in table 15.

For miscellaneous PHAST parameters that are not mentioned in table 14, input values have been chosen as described in the CEV-method (see Chapter 9).

11.2.2 Downwind deposition flux profiles

The results of the performed sensitivity analyses are presented in 'downwind deposition flux profiles'. The deposition flux profiles have been created by calculating the dry and wet deposition flux as described in paragraph 9.3 and 9.4 for the following downwind distances:

25 m	150m	700m	1300m
50m	200m	800m	1400m
60m	300m	900m	1500m
75m	400m	1000m	2000m
90m	500m	1100m	2500m
100m	600m	1200m	3000m

Sensitivity analyses have been performed by determining the downwind deposition flux profiles for a range of different input values of a certain parameter. The results of the sensitivity analyses are presented by showing the different deposition flux profiles for the range of input values in one figure.

For the dry deposition flux the deposition velocity is chosen to be $10^{-2} \text{ m}\cdot\text{s}^{-1}$. For the wet deposition flux the rain intensity is chosen to be $4\text{mm}\cdot\text{h}^{-1}$, because this value is both representative for moderate rain and moderate shower (NRPB, 1986). Figure 22 is the resulting downwind deposition flux profile when using the default values given in table 14 as input.

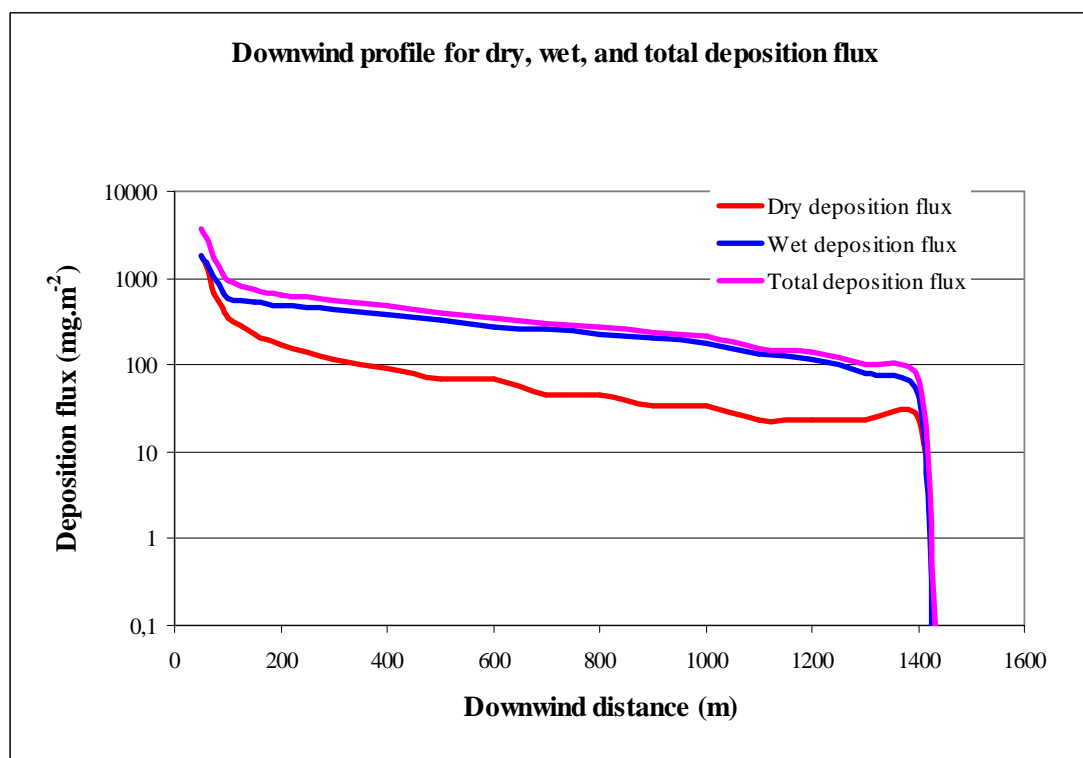


Figure 22. Downwind deposition flux profile for dry, wet and total deposition for default values using the CEV-method with PHAST.

11.3 Sensitivity analysis with OPS-ST

OPS-ST has been selected for the sensitivity analyses for:

- Plume rise
- Particle size distribution

OPS-ST is not able to present deposition fluxes as a consequence of wet deposition. Therefore sensitivity analyses have only been performed for dry deposition fluxes.

11.3.1 Default input values

The default values for all the parameters available in OPS-ST are shown table 16.

Table 16. Default input parameter values for sensitivity analyses with OPS-ST

<i>Input Parameter</i>	<i>Default value</i>
Release rate	0.16kg.s ⁻¹
Source height	0.5 m
Source diameter	25m
Heat capacity	0 MW
Receptor roughness	0.1 m
Height of wind stillness (z0)	0.1 m
Particle size distribution	Medium
Weather stability class	D
Wind speed	6m.s ⁻¹

For the parameters 'release rate', 'atmospheric stability', and 'wind speed' the default input values that have been chosen are the same as the values chosen in the sensitivity analyses performed with PHAST.

The 'source height' is chosen to be 0.5m, because it is assumed the fire is close to the ground.

A 'source diameter' of 25m has been chosen, because the fires in the CEV-method is regarded as 'not fully developed' (see paragraph 9.2.1) and the building on fire has a maximum surface of 50 x 50m (see paragraph 9.2.2).

Heat capacity is determinant for the plume rise. Therefore its default value is chosen to be 0 MW, because in the CEV-method it is assumed that plume rise is zero (see paragraph 9.1.1)

The default 'particle size distribution class' is chosen to be 'medium', because in general air pollution modelling this class represents an average particle size distribution (Van Jaarsveld, 2004).

It is chosen not to perform sensitivity analyses for receptor roughness and height of wind stillness. Therefore for both parameters a minimal value of 0.1m has been chosen, so that their influence on the OPS-ST model outcome would also be minimal.

11.3.2 Downwind deposition flux profiles

OPS-ST is able to calculate dry deposition concentration at any receptor coordinate point of interest. The dry deposition flux profiles have been made by choosing receptor point coordinates lying in the central wind axis of the modelled plume and presenting the deposition concentration at each receptor point in one graph. The resulting graph for the deposition flux profile with the OPS-ST default input values is comparable with the default deposition flux profile made with PHAST, see figure 23.

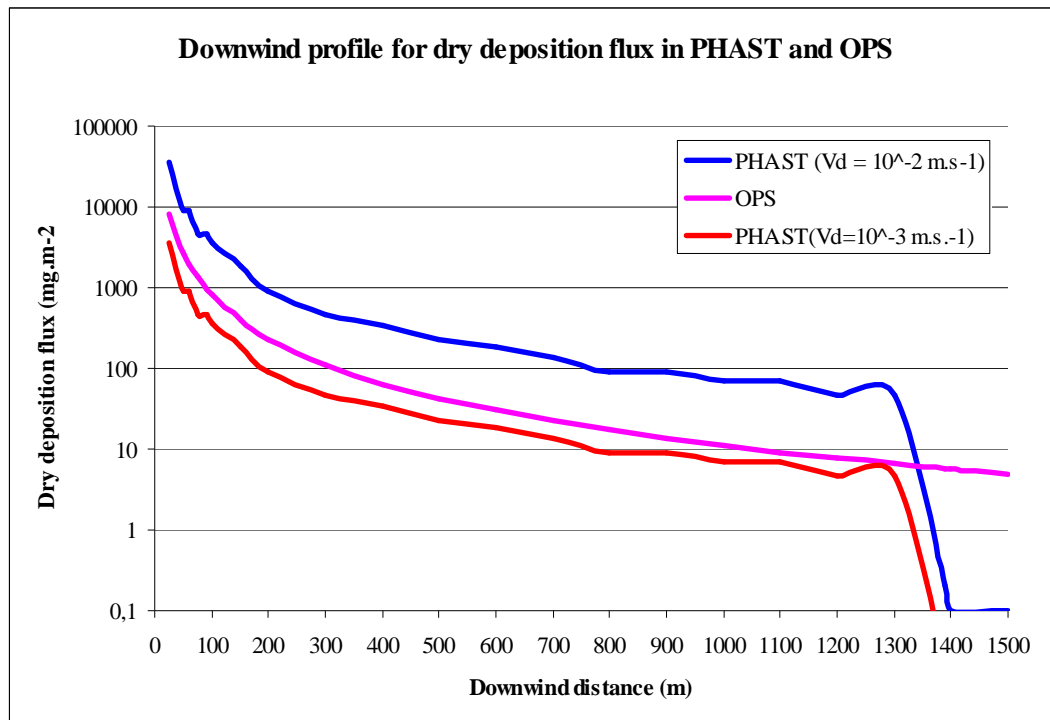


Figure 23. Downwind deposition flux profile for default input values modelled with OPS-ST compared with downwind deposition flux profile range for default input values using the CEV-method with PHAST.

Sensitivity analyses performed with PHAST

12.1 Release rate

The method prescribes a rule of thumb for different release rates based on the size of the fire and the storage of nitrogen rich products as given in table 15 in paragraph 11.2.1 The input range for the sensitivity analysis is based on these values and their average value of 0.16 kg.s^{-1} .

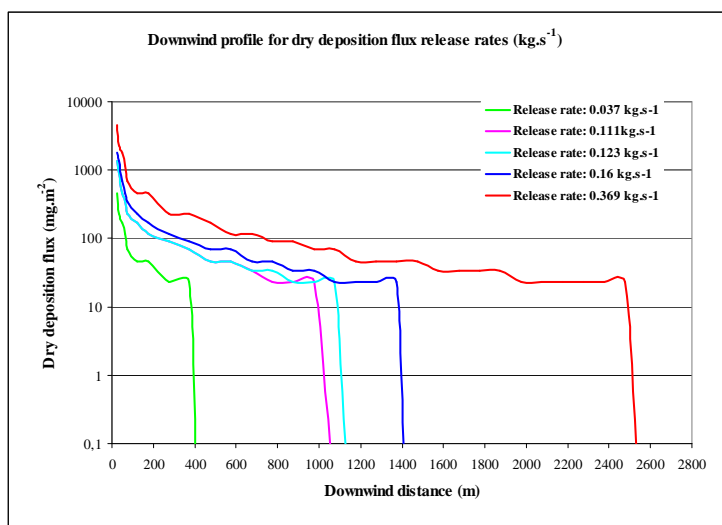


Figure 24. Sensitivity of the parameter 'release rate' on the dry deposition flux as determined by the CEV-method with PHAST.

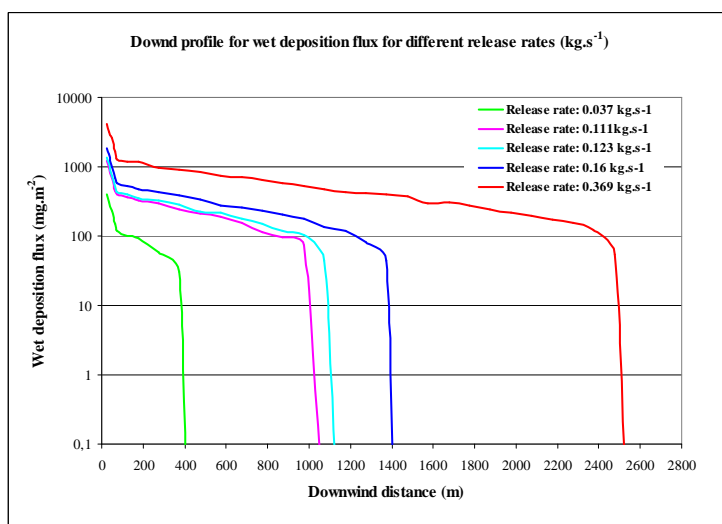


Figure 25. Sensitivity of the parameter 'release rate' on the wet deposition flux as determined by the CEV-method with PHAST.

Figure 24 and 25 show release rate is a parameter with a positive effect on both dry and wet deposition. An increase in release rate leads to an increase in dry and wet deposition flux. The input uncertainty is linear to the output uncertainty, because the multiplication of the input value for release rate, leads to an equal multiplication in the dry and wet deposition flux.

12.2 Pre-dilution air rate

Pre-dilution air rate is only relevant in case of a large amount of pre-mixed air (BOT-mi, 2010). Therefore it is chosen to compare a pre-dilution air rate of a factor 100 (100 times more air than substance) with the default pre-dilution air rate of zero. The results are given in figure 26 and 27.

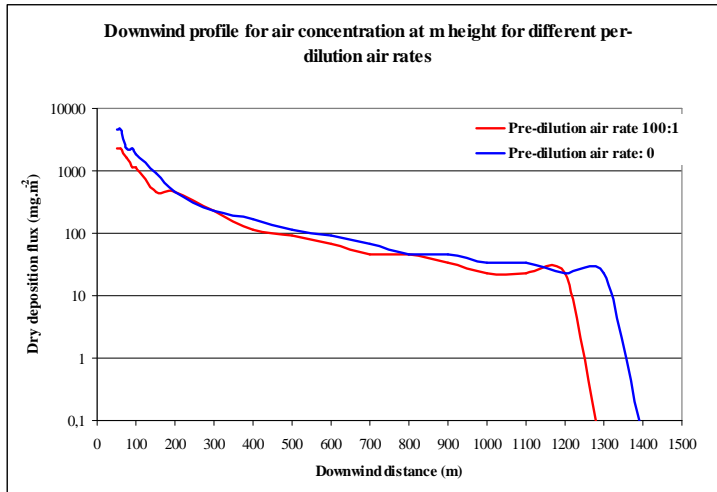


Figure 26. Sensitivity of the parameter 'pre-dilution air rate' on the dry deposition flux as determined by the CEV-method with PHAST.

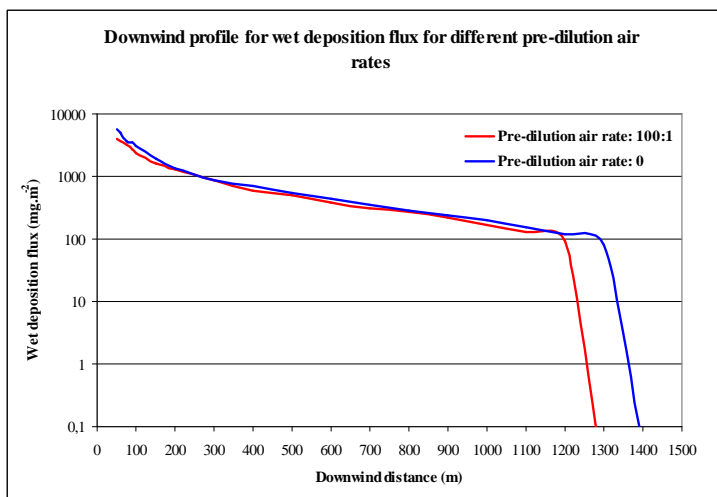


Figure 27 Sensitivity of the parameter 'pre-dilution air rate' on the wet deposition flux as determined by the CEV-method with PHAST.

Figure 26 and 27 show pre-dilution air rate is a parameter with a negative effect on both dry and wet deposition. An increase in pre-dilution air leads to a decrease in dry and wet deposition flux. The input uncertainty is narrowing the output uncertainty, because the strong multiplication of the input value for pre-dilution air rate, leads to a minimal reduction in the dry and wet deposition flux.

12.3 Final release temperature

For the sensitivity analysis of final release temperature the minimum temperature of -163°C (=110°K) in PHAST, the default temperature of 50°C (=323°K), and the maximum temperature in PHAST of 626°C (= 899°K) have been chosen.

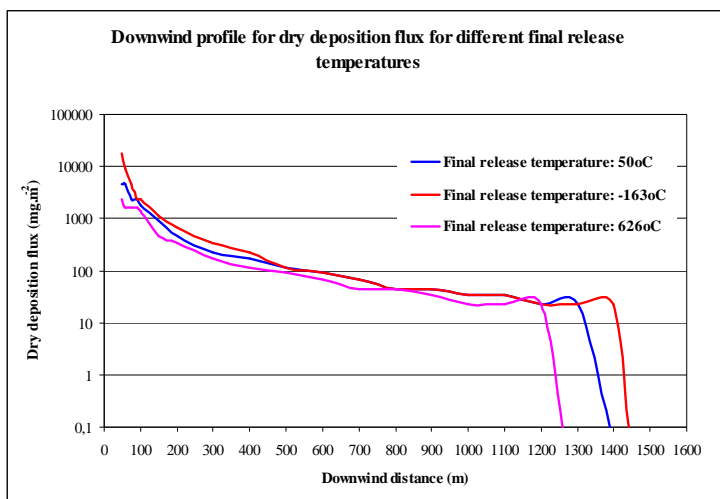


Figure 28. Sensitivity of the parameter 'final release temperature' on the dry deposition flux as determined by the CEV-method with PHAST.

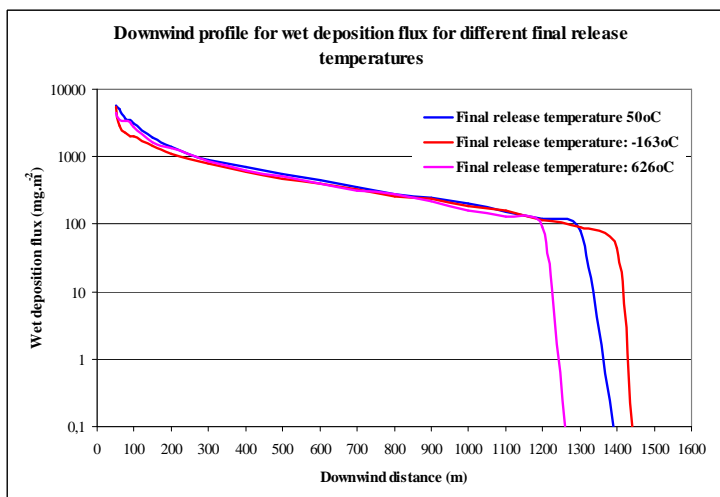


Figure 29. Sensitivity of the parameter 'final release temperature' on the wet deposition flux as determined by the CEV-method with PHAST.

Figure 28 and 29 show final release temperature is a parameter with a negative effect on both dry and wet deposition. An increase in final release temperature leads to a decrease in dry and wet deposition flux. The input uncertainty is narrowing the output uncertainty, because a strong multiplication of the input value for final release temperature, leads to a minimal reduction in the dry and wet deposition flux.

12.4 Atmospheric stability and wind speed

For the sensitivity analysis on atmospheric stability, classes A,D, and E have been chosen, because they represent unstable, neutral and stable conditions. For each stability class the most representative wind speed has been chosen.

Table 17. Input range in stability class and corresponding wind speed

Stability Class	Wind speed
A	1.5 m.s ⁻¹
D	6 m.s ⁻¹
E	3.5 m.s ⁻¹

The deposition flux profiles are given in figure 30 and 31.

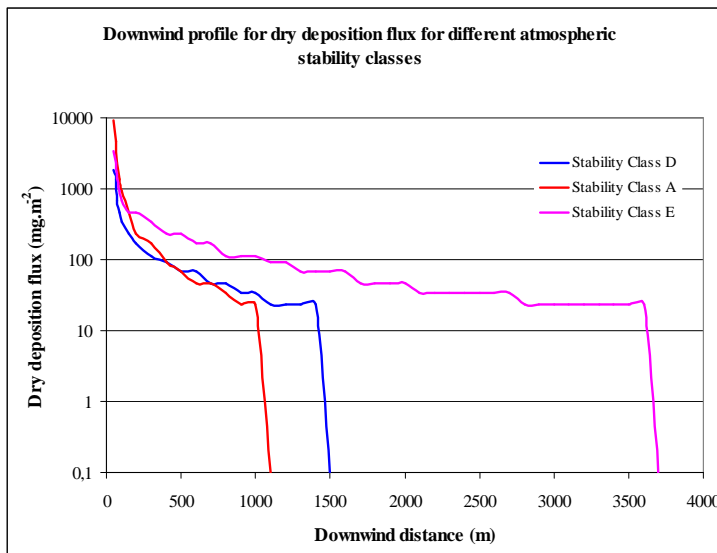


Figure 30 Sensitivity of the parameter 'atmospheric stability' on the dry deposition flux as determined by the CEV-method with PHAST.

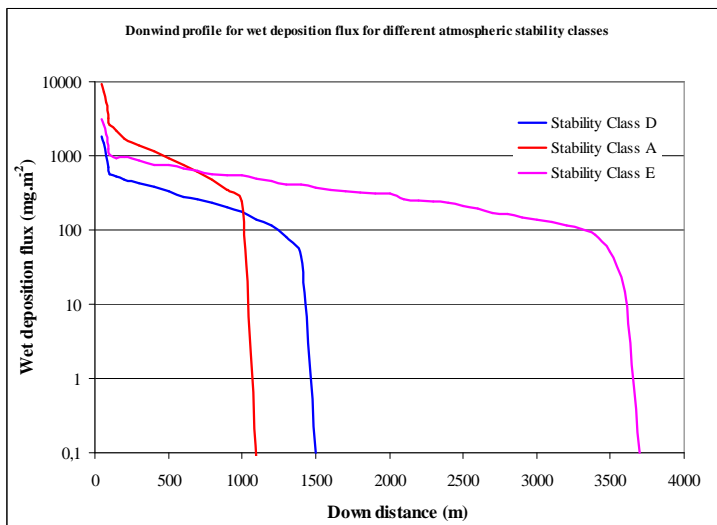


Figure 31. Sensitivity of the parameter 'atmospheric stability' on the wet deposition flux as determined by the CEV-method with PHAST.

Figure 30 and 31 show atmospheric stability is a parameter that alters both dry and wet deposition fluxes as a function of downwind distance: close to the source an unstable atmosphere (class A) has an increasing effect on dry and wet deposition flux, at distance from the source an unstable atmosphere has a decreasing effect on the dry and wet deposition flux. Compared to neutral atmospheric stability (class D) a stable atmosphere (class E) leads to an increase dry and wet deposition flux close to the source as well as at distance from the source. Input uncertainty in atmospheric stability can be considered to have a broadening effect on the output uncertainty, because the atmospheric stability class has a relative large influence in the dry and wet deposition flux.

12.5 Building dimensions

The downwind profiles for wet and dry deposition fluxes have been made for a range of building sizes with different height, broadness and surface. The values in table 18 are derived by dividing or multiplying default input values for height and width with a factor 2 or 4, see table 18.

Table 18. Input value range in sensitivity analysis on building dimensions height, width and surface perpendicular to the wind direction.

<i>Height</i>	<i>Width</i>	<i>Surface size</i>
3 m	25 m	75 m ²
3 m	50 m*	150 m ²
6m*	50 m*	300 m ² *
12 m	50 m*	600 m ²
24 m	50 m*	1200 m ²
6 m	25 m	150 m ²
6 m*	100 m	600 m ²
6 m*	200 m	1200 m ²
24 m	200 m	4800 m ²

* Default input values

In figure 32 and 33 the sensitivity analysis results are given for the input values mentioned in table 18.

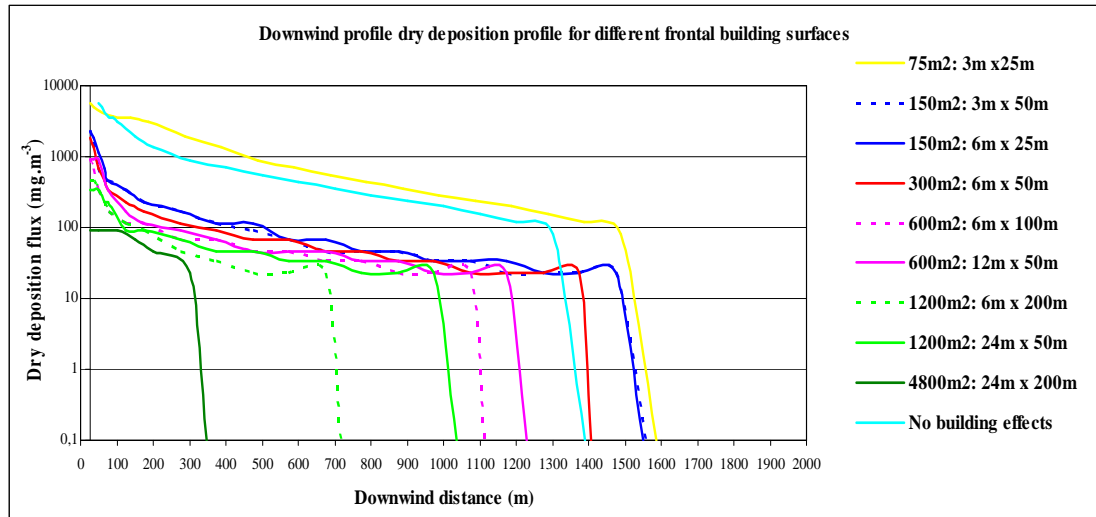


Figure 32. Sensitivity of the parameter 'building dimensions' on the dry deposition flux as determined by the CEV-method with PHAST.

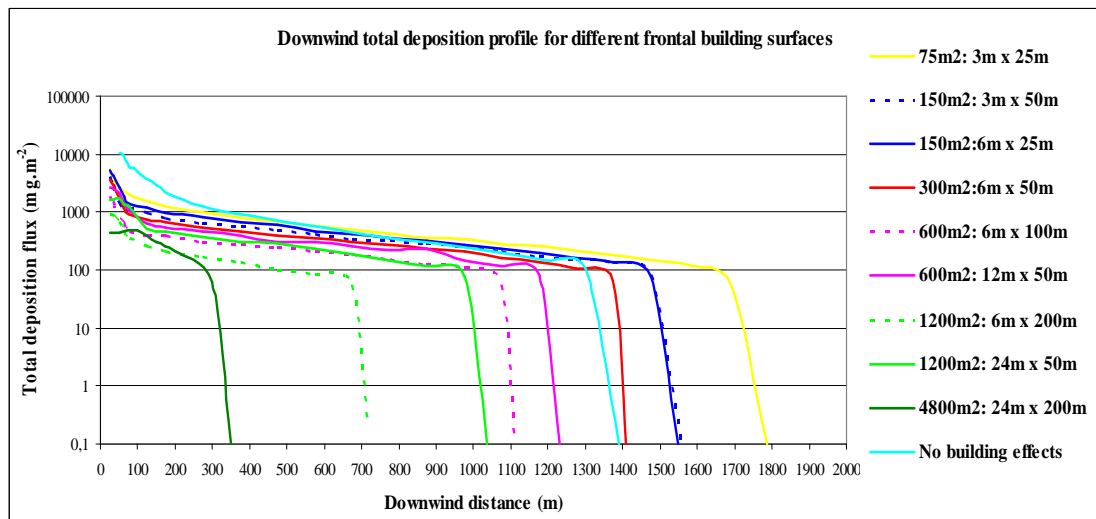


Figure 33. Sensitivity of the parameter 'building dimensions' on the wet deposition flux as determined by the CEV-method with PHAST.

Figure 32 and 33 show building surface size is a parameter with a negative effect on both dry and wet deposition. An increase in building surface leads to a decrease in dry and wet deposition flux. This influence is weaker for relative high buildings. The input uncertainty can be considered to be broadening the output uncertainty, because a multiplication of the input values for building surface leads to strong reduction in the dry and wet deposition flux.

13 Sensitivity analyses performed with OPS-ST

13.1 Plume rise

The sensitivity analysis for 'plume rise' has been performed with OPS-ST. A value for plume rise cannot be inserted directly in OPS-ST, it must be derived from the value for heat capacity (Q_h), buoyancy factor (F_b) and wind speed (u_{st}). In neutral and convective conditions OPS-ST uses the formulas 17, 18, 19 in order to determine plume rise height.

$$\Delta h = 38.8 \frac{F_b^{3/5}}{u_{st}} \quad \text{for } F_b \geq 55$$

Formula 17. (Van Jaarsveld, 2004).

$$\Delta h = 21.1 \frac{F_b^{3/4}}{u_{st}} \quad \text{for } F_b < 55$$

Formula 18. (Van Jaarsveld, 2004).

$$F_b = 8.8 Q_h$$

Formula 19. (Van Jaarsveld, 2004).

Based on the formulas above heat capacity and buoyancy factor as a function of plume rise can be described as:

$$Q_h = \frac{F_b}{8.8} = \frac{\left(\frac{\Delta h}{38.8} \cdot u_{st} \right)^{\frac{5}{3}}}{8.8} \quad \text{for } F_b \geq 55$$

Formula 20: Heat capacity as a function of plume rise for high buoyancy factor

$$Q_h = \frac{F_b}{8.8} = \frac{\left(\frac{\Delta h}{21.1} \cdot u_{st} \right)^{\frac{4}{3}}}{8.8} \quad \text{for } F_b < 55$$

Formula 21: Heat capacity as a function of plume rise for low buoyancy factor

In the OPS-ST-model the horizontal location of the final (and maximum) plume rise (x_f) is assumed to be zero, because OPS originally is a long-term emission dispersion model. Under the assumption that on average the vertical rise goes faster than the (downward) vertical plume growth, the final plume rise in the OPS-ST-model is considered to be instantaneously reached (Van Jaarsveld, 2004). Formulas 22 and 23 are based on the Briggs' Equations, and are equal to the formulas mentioned in the logic diagram proposed by Beychock (figure 7, paragraph 5.2.). When applying the formulas from Beychocks diagram the horizontal distance of maximum plume rise lacking in the OPS-ST-model could be described as:

$$x_f = 119(F_b)^{0.40} \text{ for } F_b \geq 55$$

Formula 22: Horizontal distance of maximum plume rise as a function of high buoyancy factor (Beychock, 2005).

and

$$x_f = 49(F_b)^{0.625} \text{ for } F_b < 55$$

Formula 23: Horizontal distance of maximum plume rise as a function of low buoyancy factor (Beychock, 2005).

In modelling plume dispersion for an incidental emission such as a fire, horizontal location of the final and maximum plume rise x_f is crucial, but in the OPS-ST-model x_f is missing. The results of the sensitivity analysis should therefore be regarded as indicative. In order to be able to discuss the results in a proper context the missing x_f values are presented for every plume rise height.

13.1.1 *Inserted values*

The following plume rise heights (and corresponding heat capacity, buoyancy factor and horizontal distance of maximum plume rise) are chosen for the sensitivity analysis.

Table 19. Input range for plume rise heights and the corresponding buoyancy factors, heat capacities and horizontal distances of maximum plume rises.

<i>Plume rise height (Δh)</i>	<i>Buoyancy Factor*¹ (F_b)</i>	<i>Heat capacity (Qh)*^{1,2}</i>	<i>Horizontal distance of maximum plume rise (x_f)*^{1,3}</i>
0 m	0 m ⁴ .s ⁻³	0 MW	0 m
1 m	0.19 m ⁴ .s ⁻³	0.02 MW	17 m
2 m	0.47 m ⁴ .s ⁻³	0.05 MW	31 m
5 m	1.60 m ⁴ .s ⁻³	0.18 MW	66 m
10 m	4.02 m ⁴ .s ⁻³	0.46 MW	117 m
25 m	13.7 m ⁴ .s ⁻³	1.55 MW	251 m
71 m	55 m ⁴ .s ⁻³	6.22 MW	598 m

*1 The inserted heat capacity and buoyancy factor values have been derived from the formula 20 and 21, with $u_{st} = 6 \text{ m.s}^{-1}$. x_f is derived from the formulas 22 and 23.

*2 Heat capacity is the actual input parameter in OPS-ST

*3 Horizontal distance of maximum plume rise (x_f) is not modelled with OPS-ST

The sensitivity analysis has been performed with particle size distribution class 'medium', an emission rate of 160 g.s⁻¹, neutral atmospheric stability (class D), and a wind speed of 6 m.s⁻¹.

13.1.2 Dry deposition flux profiles for different plume rise heights

For the different plume rise heights the dry deposition flux has been derived as described in paragraph 11.3. The results are shown in figure 34 and table 20.

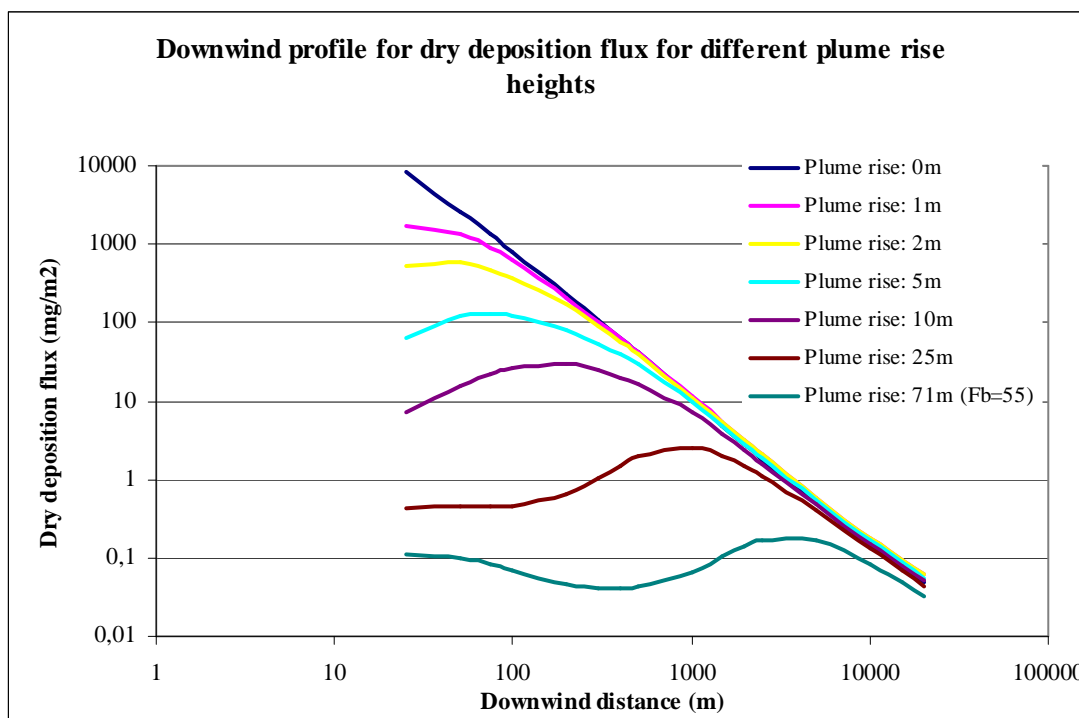


Figure 34. Sensitivity of the parameter 'plume rise' on the dry deposition flux as determined with OPS-ST.

Table 20. Dry deposition flux per downwind distance as a function of plume rise height.

	Dry deposition flux (mg.m ⁻²) for different plume rise height						
	0m	1m	2m	5m	10m	25m	71m
25m	8308.9	1740.3	526.5* ¹	63.4* ¹	7.1* ¹	0.4* ¹	0.1* ¹
50m	2659.5	1336.6	605.4	118.3* ¹	15.6* ¹	0.5* ¹	0.1* ¹
75m	1325.5	900.6	483.2	131.2	22.4* ¹	0.4* ¹	0.1* ¹
100m	802.2	620.9	373.4	124.9	26.8	0.5* ¹	0.1* ¹
200m	232.0	211.1	169.2	80.6	29.4	0.7* ¹	0.0* ¹
300m	109.7	104.6	90.6	52.9	24.7	1.1	0.0* ¹
400m	64.5	63.1	56.6	39.3	20.0	1.5	0.0* ¹
500m	42.5	42.3	38.9	29.4	16.3	2.0	0.0* ¹
1000m	11.0	11.6	11.2	9.6	7.2	2.6	0.1
1500m	4.9	5.4	5.3	4.8	3.8	2.0	0.1
2000m	2.8	3.2	3.1	2.9	2.4	1.5	0.1
2500m	1.8	2.1	2.1	1.9	1.6	1.1	0.2
5000m	0.5	0.6	0.6	0.5	0.5	0.4	0.2
10000m	0.2	0.2	0.2	0.2	0.2	0.1	0.1
15000m	0.1	0.1	0.1	0.1	0.1	0.1	0.0
20000m	0.0	0.1	0.1	0.1	0.1	0.0	0.0

*¹ within distance of virtual horizontal distance of maximum plume rise (x_f)

Figure 34 and table 20 show plume rise is a parameter with a negative effect on dry deposition. An increase in plume rise leads to a decrease in dry deposition flux. Plume rise also changes the dry deposition fluxes as a function of downwind distance. For relative small plume rise heights (1-10m) the dry deposition flux is increasing with the downwind distance until a maximum has been reached close to the source (within 0-200m). For relative large plume rise heights (25-71m) the dry deposition flux first decreases with the downwind distance until a minimum has been reached, then the dry deposition increases until a maximum has been reached. For all plume rise heights it applies that after the maximum has been reached, the dry deposition flux decreases with the downwind distance. At very large distance from the source (>10 km) the influence of plume rise height on the dry deposition flux is very small. It can be considered that the input uncertainty is broadening the output uncertainty, because a minor multiplication of the input value for plume rise, could lead to a strong reduction in dry deposition flux, especially for distances close to the source and relative low plume rise heights.

13.2 Particle size distribution

For the sensitivity analysis of particle size distribution the general distribution classes fine, medium, and coarse have been selected as well as two classes representing typical particle size distributions for particles formed in a fire. The general class distributions are already included in OPS-ST and are given in table 21. The particle size distribution is given by the mass fraction of different particle size ranges. The mass mediated diameter represents the particle size range in the OPS-ST-model.

Table 21. Particle size distribution for classes fine, medium, and coarse applied in OPS-ST (Van Jaarsveld, 2004).

<i>Particle size range</i>	<i>Mass mediated diameter</i>	<i>Mass fraction (%) for class fine</i>	<i>Mass fraction (%) for class medium</i>	<i>Mass fraction (%) for class coarse</i>
<0.95 μm	0.5 μm	70	53.0	42
0.95-2.5 μm	1.55 μm	20	19.8	22.7
2.5-4 μm	3.2 μm	2.75	8.2	10.3
4-10 μm	6.2 μm	2.75	11.5	14.5
10-20 μm	13.6 μm	2.5	4.2	5.9
>20 μm	50 μm	2.0	3.3	4.6

It is not possible yet to predict particle size distribution in a fire, but a typical diameter for a particle formed in fire is 1 μm (Stec &Hull, 2010). Data-fits performed by Butler & Mulholland, show the geometric standard deviation could differ from 2 to 16 (Butler & Mulholland, 2004). Based on these statements two particle size distributions have been made, according to a lognormal distribution with the geometric average of the particle diameter assumed to be 1 μm , and geometric standard deviations (σ) of 2 and 16. Based on the lognormal distribution the mass fractions are calculated and are given in table 22.

Table 22. Particle size distribution for two indicative fire specific classes with a geometric averaged particle diameter size of 1 μm ($\mu = 1 \mu\text{m}$) and geometric standard deviations of 2 and 16 ($\sigma=2$ and $\sigma=16$).

Particle size range	Mass mediated diameter	Mass fraction (%) for $\sigma =2$	Mass fraction (%) for $\sigma =16$
<0.95 μm	0.5 μm	30	47.3
0.95-2.5 μm	1.55 μm	18.4	2.4
2.5-4 μm	3.2 μm	9.3	1.2
4-10 μm	6.2 μm	16.6	2.3
10-20 μm	13.6 μm	9.8	1.7
>20 μm	50 μm	5.9	45.0

Figure 35 displays the deposition flux profiles for the different particle size distributions.

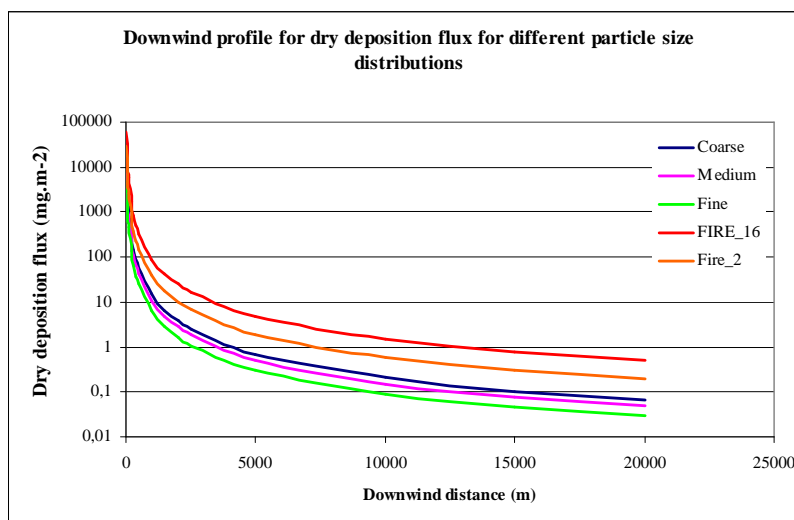


Figure 35. Sensitivity of the parameter 'particle size distribution' on the dry deposition flux as determined with OPS-ST. Particle size distribution in classes FIRE_2 and FIRE_16 are based on a geometric average particle diameter of 1 μm ($\mu = 1 \mu\text{m}$) and a geometric average of respectively 2 ($\sigma=2$) and 16 ($\sigma=16$).

Figure 35 shows particle size has a positive effect on dry deposition. An increase in the mass-fraction representing large particles (>20 μm) will lead to an increase in dry deposition flux. Input uncertainty can be considered to be broadening the output uncertainty, because an increase in the mass-fraction of large particles leads to a strong increase in dry deposition flux. (Note that the y-axis representing the dry deposition flux in figure 35 has a logarithmic scale.)

14 Discussion

14.1 Consequences of input uncertainty for parameters

14.1.1 Release rate

The results of the sensitivity analysis show that within the chosen input range the input uncertainty has a linear influence on the output. These results however should be regarded as indicative, because it is assumed that the chosen input range for 'nitrogen dioxide release' also applies for 'particle release'.

Table 6 in paragraph 9.2.1 illustrates that the actual input values for release rate of particles are uncertain. Release rate is determined by the burning rate, fire size and particle emission factor of the fuel. In the CEV-method the burning rate is assumed and the fire size estimated by the building dimensions. Emission factors are only known for a few materials, while during a fire several fuels are being burned simultaneously. Table 6 shows that the emission factor per fuel could differ from 2 g/kg fuel (wood) to 130 g/kg fuel (oil), which indicates the difference in order of magnitude between particle emission factors per fuel.

In theory the uncertainty in release rate should be manageable, because the uncertainty in the input is linear to the uncertainty in the output. Release rate however is a very important dispersion parameter. Predictive dispersion and deposition concentration are therefore still uncertain.

14.1.2 Building dimensions

The sensitivity analysis performed with PHAST shows that the dispersion is very sensitive for the size of the buildings frontal surface. Input uncertainty for this parameter is small, because in case of a PGS-15 fire the size of the building is well-known until the moment of roof collapse (InfoMil, 2007). A roof collapse could change the building dimensions but, after roof collapse it is assumed no hazardous concentrations at residential height will be present, because the fire is then in its free-burning stage causing the smoke plume to rise (BOT-mi, 2010). Therefore uncertainty in building dimensions is only relevant in case of a miscellaneous fire with unknown building dimensions and a scenario where plume rise does not occur after roof collapse.

14.1.3 Pre-dilution air rate

Based on pasted experiences by the CEV it is already recognized in the CEV-method that pre-dilution air rate is only relevant in case of large amounts of pre-mixed air (BOT-mi, 2010). This has been confirmed by the sensitivity analysis performed with PHAST.

14.1.4 Final release temperature

The sensitivity analysis performed with PHAST shows that final release temperature is a parameter with relative little sensitivity. Also the assumed release temperature of a cold jet plume of 50°C in the 30 minutes before roof collapse in PGS-15 warehouses (BOT-mi, 2010) is well underpinned and plausible. Moreover the small sensitivity of this parameter narrows the input uncertainty for miscellaneous fires.

Final release temperature however, must not be confused with heat input. When applying the CEV-method final release temperature is determinant for the dispersion of the released cloud of exemplary substance nitrogen: a high release temperature results in a high difference with the ambient air temperature, causing a faster dilution process. Heat input is determinant for the buoyancy factor and plume rise, which uncertainty and sensitivity is discussed in paragraph 14.1.6.

14.1.5 *Atmospheric stability*

In the CEV-method an atmospheric stability class and wind speed is chosen based on meteorological measurements are provided by the Royal Dutch Meteorological Institute (BOT-mi, 2010). There is little uncertainty about the stability class and wind speed being chosen correctly. However detailed information (such as changing wind direction, and local differences in wind speed, exact Monin-Obukhov length) is lost by categorizing in stead of parametrizing the atmospheric stability and wind speed. This could result in a minor uncertainty of the plume dispersion within a certain atmospheric stability class. Because of a relative large sensitivity for atmospheric stability, uncertainty in predicting the dispersion and dilution of the plume is notable.

14.1.6 *Plume rise*

Plume rise causes major uncertainty in predicting dispersion and deposition of particles released in a fire, because it both has a large sensitivity and input uncertainty. The CEV-method deals with this uncertainty by choosing only to perform prediction for fire scenarios with no plume rise (e.g. the first 30 minutes in PGS-15 fires). However even in these scenarios plume rise may still cause uncertainty in the predicted outcome, because in every fire it can be expected a source of heat is present causing at least some minor plume rise (1-5m). The sensitivity analysis showed that the sensitivity is very large for those heights, especially at distances close to the fire. The sensitivity analysis results on plume rise however should be regarded as indicative, because the applied model OPS-ST is developed for other purposes than performing sensitivity analyses on plume rise. A difference in plume rise height between 1-5m is considered to be relatively small since OPS-ST is not developed to model with such small values. Experts state that this may influence the accuracy of the performed sensitivity analysis. Also OPS-ST assumes the final plume rise is reached instantaneously, whereas in reality the horizontal location of the final plume rise is at a downwind distance determined by the wind speed and the plumes' buoyancy factor. However the sensitivity that is found with OPS-ST is very large. This indicates that despite the possible inaccuracies of OPS-ST plume rise is a sensitive parameter. This causes uncertainty in the prediction of particle deposition and dispersion, especially for distances close to the fire. The assumption in the CEV-method that plume rise height is 0, could cause major overestimation of the predicted dry deposition.

14.1.7 *Particle size distribution*

Particle size distribution is determinant for the deposition velocity, but it cannot be predicted based on fuel and fire conditions. In the CEV-method it is therefore assumed that the deposition velocity is within the range of 10^{-3} and 10^{-2} m.s⁻¹ (BOT-mi, 2010). Figure 36 compares the resulting deposition fluxes from this range with the deposition fluxes for fine, medium, coarse and two indicative particle size distributions for particles formed in a fire.

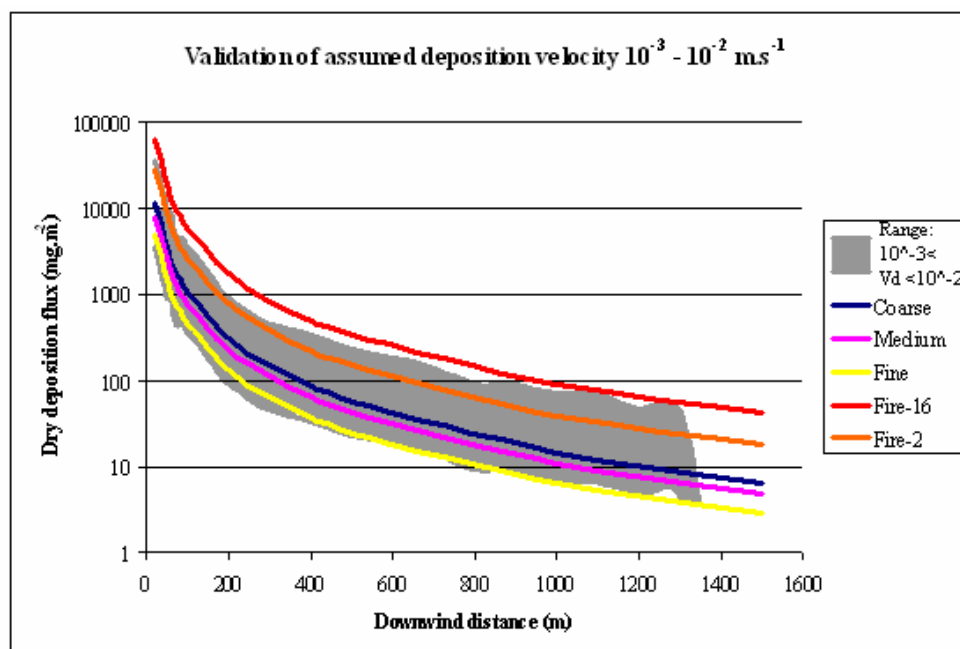


Figure 36. Comparison of dry deposition flux for different particle size distribution with the deposition flux as determined in the CEV-method with PHAST and an assumed deposition velocity between 10^{-3} and 10^{-2} m.s^{-1} .

The range suffices for the general size distribution classes fine, medium, and coarse, but if during a fire particle sizes are distributed with a relative large geometric standard deviation ($\sigma = 16$), it could be possible that the deposition flux is (slightly) underestimated. The interpretation of the size distribution for particles formed in a fire however is based on the assumption that the geometric average diameter is $1 \mu\text{m}$ and when determining the particle size distribution a correct geometric average diameter is crucial. The results on the deposition fluxes for the size distribution for particles formed in a fire should therefore be regarded as indicative.

14.2 No sensitivity analyses on source term parameters

The critical review has shown that many source term emission parameters or not included or indirectly included in the CEV-method, see paragraph 10.2. However it is chosen not to perform sensitivity analyses on these parameters, because a suitable model is not available. In 2009 Mennen and co-authors have performed a survey on models for the dispersion of compounds released by fires. They concluded that only model would be of actual added value in predicting source term emission: FIREPEST developed by the Health and Safety Executive (HSE) of Great Britain (Mennen et al, 2009). However the HSE does not supply this model to third parties and is therefore unavailable. This is why no sensitivity analyses have been performed for the source term emission parameters mentioned in paragraph 10.2.

14.3 No sensitivity analyses performed on inversion layer height

'Inversion layer height' is only relevant in case the plume rise is so high it is able to reach the inversion layer. Inversion layer heights are at 50 to 1500m and the results on plume rise have shown that in case of a plume rise of 50m deposition concentrations are already very much diluted. It is therefore chosen not to perform a sensitivity analysis on inversion layer height.

14.4 Personal interpretation in choosing concentration layer values for PHAST sideview graphs

Paragraph 9.3 describes there is no straightforward method in choosing representative values for the concentration layers in the PHAST sideview graphs. However the sensitivity analyses on the parameters 'release rate', 'building dimensions', 'pre-dilution air rate', 'final release temperature' and 'atmospheric stability' have been performed with PHAST and their deposition flux profiles are based on PHAST sideview graphs. This means the sensitivity analysis results are partially based on a personal interpretation for 'representative concentration layer values'. In the sensitivity analyses, each determined deposition flux profile is based on at least 10 different concentration layers. The stepsize differences between the chosen concentration values for these layers are also never larger than 50%. Because of this thorough method of interpreting the PHAST sideview graphs, no large misinterpretations of the sideview graphs are expected. The deposition flux profiles could be more precise, but they serve their goal in representing the sensitivity of a parameter in PHAST.

14.5 Release of heavy metals in fires

Heavy metals are not formed in a fire, but they could be released in a fire because they are present in the fuels. However there has no scientific literature found that describes this process in detail.

14.6 Nanosized particles released in a fire

Paragraph 7.2 describes health effects as a function of the size distribution of inhaled particles. The most health concern is for nanosized particles (< 0.1µm), because they are able to penetrate more deeply into the lungs (Madl et al, 2010) and are more difficult to be removed by macrophages (Kreyling et al, 2004).

Chapter 4 describes that primary particles formed in a fire are nanosized (Kennedy 1997). In general these primary particles will grow in the fire environment by coagulation, agglomeration and condensation of vapours (Butler & Mulholland, 2004). This results in a typical particle size of 1 µm for smoldering

combustion and often even larger particles for flaming combustion (Stec & Hull, 2010).

Butler & Mulholland performed data-fits for the size distribution of particles released in a fire. They found the particle size distribution to be lognormal and geometric standard deviations ranges from approximately 2 to 16 (Butler & Mulholland, 2004; Mulholland, 2008). An interpretation of the lognormal distribution indicates that nanosized particles are released during in a fire in a considerable amount: when assuming the geometric average particle diameter is 1 μm and the geometric standard deviation is between 2 and 16, the mass-fraction of nanosized particles is between 5 and 40%. The data-fits performed by Butler & Mulholland however lack an independent verification (Butler & Mulholland, 2004). Also the interpretation of the data-fits is based on an assumed geometric average, which is crucial in predicting particle size distribution (Mulholland, 2008). The interpretation however indicates that it is possible that during a fire a considerable mass-fraction of nanosized particles is released.

Particle size distribution and especially the mass-fraction of nanosized particles is important for predicting health effects after inhalation. However it is not included in the CEV-method, because at the time particle size distribution cannot be predicted based on fuel chemistry and fire conditions (Mulholland, 2008). Therefore in case the CEV is asked to construct public health advice on inhalation of particles released in a fire, particle size distribution and especially the mass-fraction of nanosized particles, is an uncertainty factor.

14.7 Soil contamination by PAHs and dioxins bound to deposited particles

After a fire the surrounding soil can be contaminated by the deposition of particles released in the fire which contain hazardous substances such as PAHs and dioxins. The formation of PAHs and dioxins is promoted by poor combustion conditions with low oxygen levels and relative low combustion temperatures (Mastral & Callen, 2000; Al-Alawi, 2008).

The CEV-method is mainly focused on the first 30 minutes of a fire. At 30 minutes it is assumed that the roof collapses and the fire has developed into the free-burning stage. So for the CEV-method the fires' incipient stage and beginning of the free-burning stage are most relevant.

During the incipient stage and the beginning of the free-burning stage the fire is still fuel regulated (MAIFF, 2011). This means that in the period of 30 minutes the CEV-method is focused on, the combustion conditions are not poor, because of sufficient oxygen levels. Thus relative high mass-fractions of dioxins and PAHs are not expected on the released particles considered in the CEV-method.

15 Conclusion

During a fire (soot) particles are released possibly containing hazardous substances such as polycyclic aromatic hydrocarbons (PAHs), dioxins and heavy metals. These particles will disperse through the air and then deposit to the ground. For health reasons it is important to predict the particle concentrations in the air and the concentration of PAHs, heavy metals and dioxins on the ground. The prediction of the dispersion and deposition of particles released in a fire is complex due to uncertainties.

15.1 The CEV-method

The CEV-method predicts the particle dispersion with the consequence and risk model PHAST. The major input parameters for this model are:

- Release rate
- Building dimensions
- Pre-dilution air rate
- Final release temperature
- Atmospheric stability

The prediction of the deposition of the particles is based on the output PHAST gives in sideview graphs. Dry deposition fluxes are calculated with the formula:

$$F_{dry} = C_{air} \cdot V_d \cdot t$$

F_{dry}	=	Dry deposition flux ($\text{mg}\cdot\text{m}^{-2}$)
V_d	=	Deposition velocity ($\text{m}\cdot\text{s}^{-1}$)
C_{air}	=	Particle concentration in the air at 1m height ($\text{mg}\cdot\text{m}^{-3}$)
t	=	Release time (s)

In this formula C_{air} is derived from the PHAST sideview graph. The deposition velocity (V_d) is assumed to be between 10^{-3} and 10^{-2} $\text{m}\cdot\text{s}^{-1}$, based on recommendations of NRPB research on particle deposition.

Wet deposition fluxes are calculated with the formula:

$$F_{wet} = C_{plume} \cdot h \cdot (J / J_0) \cdot \Lambda \cdot t$$

F_{wet}	=	Wet deposition flux ($\text{mg}\cdot\text{m}^{-2}$)
C_{plume}	=	Average concentration in the air column ($\text{mg}\cdot\text{m}^{-3}$)
h	=	height of the plume (m)
J	=	rain intensity ($\text{mm}\cdot\text{hour}^{-1}$)
J_0	=	rain intensity of $1\text{mm}\cdot\text{hour}^{-1}$
Λ	=	scavenging rate (s^{-1}) of particles corresponding with a rain intensity of $1\text{mm}\cdot\text{hour}^{-1}$
t	=	release time (s)

In this formula C_{plume} and h are derived from the PHAST sideview graph. The scavenging rate corresponding with a rain intensity of $1\text{mm}\cdot\text{hour}^{-1}$ is assumed to be $4\cdot 10^{-4}\text{s}^{-1}$ based on recommendations in the Yellow Book (CPD, 2005).

15.2 Critical review on the CEV-method

In a critical review the CEV-method has been compared with the current knowledge available in scientific literature. The comparison showed that a number of source term parameters and some air dispersion parameters are not or only indirectly included in the CEV-method.

15.3 Uncertainties and their consequences

Based on the CEV-method and scientific literature the uncertainties related to important parameters have been described on a qualitative level. Sensitivity analyses have been performed in order to determine the consequences of these uncertainties on the outcome of the prediction. The parameters' uncertainties, sensitivity and their influences on the CEV-method prediction are discussed below.

Release rate: Smoke emission cannot be predicted based on fuel chemistry and fire conditions (Mulholland, 2008). In the CEV-method the release rate of particles is estimated by an assumed burning rate, an estimation of the fire size with the building dimensions, and an emission factor which is only known for few materials. Release rate is therefore a parameter with major uncertainty, but due to the linear sensitivity it is not broadened in predictions for particle dispersion and wet and dry deposition fluxes.

Plume rise: Smoke emission cannot be predicted based on fuel chemistry and fire conditions (Mulholland, 2008). The height of the emitted smoke plume cannot be modelled. The CEV therefore only performs predictions in fire scenarios with no plume rise. However in every fire at least minor plume rise can be expected and assuming the plume rise is zero causes overestimation in predicting dry deposition flux values, especially for distances close to the fire. The large sensitivity of the parameter broadens this overestimation.

Particle size distribution: Smoke emission cannot be predicted based on fuel chemistry and fire conditions (Mulholland, 2008). The size distribution of the particles in the emitted smoke is therefore uncertain. Particle size distribution is a sensitive parameter for the prediction of dry deposition fluxes, because it is determinant for the deposition velocity. The CEV-method assumes the deposition velocity is between 10^{-3} and 10^{-2} m.s⁻¹. A comparison with the sensitivity analysis results on different particle size distribution indicates the true deposition velocity is within this range.

Miscellaneous parameters that have been analyzed, such as 'building dimensions', 'pre-dilution air rate', 'final release temperature', and 'atmospheric stability' are considered to be less relevant, because the parameters are well-known or the parameter has little influence on the prediction of the dispersion and deposition of particles released in a fire.

An overview of the uncertainty, sensitivity and uncertainty consequences for each parameter is given in table 23.

Table 23. Relative input uncertainty and its consequences for major parameters in predicting dispersion and deposition of particles released in a fire.

<i>Parameter</i>	<i>Uncertainty</i>	<i>Applied model</i>	<i>Sensitivity</i>	<i>Uncertainty Consequences</i>
Release Rate	++	PHAST	+-	+
Building dimensions	-	PHAST	+	-
Pre-dilution air rate	+	PHAST	--	-
Final Release Temperature* ¹	+-	PHAST	--	-
Atmospheric Stability	-	PHAST	++	+-
Plume Rise* ¹	++	OPS-ST	++	++
Particle Size Distribution	++	OPS-ST	+	+

*1 Both plume rise and release temperature are a result of heat input. When using CEVs' current method with PHAST the release temperature is relevant for the dispersion, because of the difference in temperature of the released exemplary substance nitrogen and the ambient air, whereas in OPS-ST the heat input is used in order to determine the buoyancy factor.

15.4 Answer on the research question

“What are the consequences of the uncertainties in predicting dispersion and deposition of particles released in a fire when using the current CEV-method?”

The major uncertainties are plume rise, release rate and particle size distribution. The uncertainty on particle size distribution is manageable by assuming a deposition velocity between 10^{-3} and 10^{-2} m.s⁻¹. Because of the uncertain plume rise the CEV only performs predictions for fire scenario with no plume rise. However assuming plume rise is zero results in overestimation of predicted dry deposition fluxes. Release rate is a major uncertainty. Because smoke emission cannot be predicted based on fuel chemistry and fire conditions, the emission rate of particles, PAHs, dioxins and heavy metals can only be assumed. The CEV therefore states that any predicted deposition flux values is considered to be an estimation for the order of magnitude. For a well-constructed health advice the PHAST model result alone does not suffice, measurements are necessary also.

16 Recommendations

16.1 Recommendations for CEV-method improvement

16.1.1 *No reasons to believe the CEV-method is mathematically incorrect*

The prediction method that the CEV applies seems rather unorthodox, but within the scope of this study there are no reasons to believe the CEV-method is incorrect. The applied deposition formulas are acknowledged in scientific literature. The calculated deposition flux values based on the output of the consequence and risk model PHAST are comparable with the deposition flux values that are modelled with air dispersion model OPS-ST. Also the indicative verification provides no reason to believe that the CEV-method is mathematically incorrect.

16.1.2 *No prediction in case of visually observed plume rise*

The general CEV-approach not to perform calculations in case of visually observed plume rise seems valid. In case of a relative large plume rise particle concentrations at residential height are strongly diluted. Moreover the sensitivity of plume rise causes major uncertainty on the calculation outcomes.

16.1.3 *Deposition flux tool in PHAST*

The CEV-method predicts deposition flux by performing calculations based on PHAST output. Based on the sideview graphs the values for the necessary variables 'concentration at 1 m height' and 'air column content' are determined by a personal interpretation. This would not be necessary, if a tool is introduced in PHAST that calculates deposition directly from the sideview. With this tool the CEV-method takes less time, is more accurate and is easier to perform.

16.2 Recommendations for further research

16.2.1 *The interaction between plume rise and inversion layer height*

In this study it was chosen not to perform sensitivity analyses for 'inversion layer height'. Dependent on the atmospheric stability inversion layer heights are between 50 and 1500m (Van Jaarsveld, 2004). In order to perform a sensitivity analysis on 'inversion layer height' a plume rise of at least 50m during very stable atmospheric conditions is therefore necessary. The sensitivity analyses on plume rise showed that dry deposition fluxes decrease with an increasing plume rise height. For plume rise heights larger than 50m, dry deposition flux concentrations are probably too small for a sensitivity analysis on inversion layer height. However this does not mean that 'inversion layer height' cannot be a relevant parameter in certain scenarios. Paragraph 5.4 describes a scenario of a smoke plume trapped under the inversion layer (Bluet et al, 2004). In the sensitivity analysis on plume rise a release rate of $160 \text{ g}\cdot\text{s}^{-1}$ is chosen. With a larger release rate the dry deposition fluxes may not be too small for the performance of sensitivity analysis. A recommendation for further research is therefore to perform sensitivity analyses on the interaction between plume rise and inversion layer height for fires with a larger release rate.

16.2.2 *Size distribution of particles formed in a fire*

Particle size distribution is determinant for the deposition velocity and is therefore an important parameter for the dry deposition flux. Particle size distribution is also important for the air quality, because it is determinant for the amount of nanosized particles and there is great health concern for inhalation of nanosized particles. However particle size distribution cannot be predicted based on fuel chemistry and fire conditions (BOT-mi, 2010; NRPB, 1983). The deposition velocities applied in the CEV-method are indirectly based on general particle deposition studies with 'general' particle size distributions. A recommendation for further research is therefore to investigate if the size distribution of particles formed in a fire is significantly different compared to particle size distributions in general particle deposition studies. This way it can be checked if the assumed deposition velocities in the CEV-method are correct. Also it can indicate if there should be more health concern on inhaling (nanosized) particles released in fire.

16.2.3 *Modelling source term parameters with FIREPEST*

In the CEV-method uncertainties are recognized for source term parameters resulting in a major uncertainty in release rate. The model FIREPEST from HSE is able to model important parameters that determine the release rate, e.g. fire size, fire duration, release rate of hazardous substances, burning rate, fire temperature, the state of the building during a fire, and outflow as a result of building dimensions. The HSE however does not supply this model to third parties, and the model is therefore unavailable to the CEV. The CEV could ask the HSE to perform estimations on the released for a number of standard fire scenarios. Also sensitivity analyses on the FIREPEST parameters would give more insight on the uncertainty that is related to release rate.

17 Literature

Al-Alawi, M. 2008. Dioxin characterization, formation, and minimisation. The fate of persistent organics pollutants in the environment, pages 269-282. Springer, 2008.

Bakkum, E.A. 1993. Een numeriek algoritme voor de berekening van droge depositie en uitwassing van emissies in de atmosfeer. TNO-IMET report 93-211, TNO, 1993.

Bankston, C. P., Powell, E. A., Cassanova, R. A., Zinn, B. T., J. 1977. Fire Flammation. Volume 8, page 395.

Bankston, C. P., Cassanova, R. A., Powell, E. A., Zinn, B. T. 1978. Review of Smoke Particulate Properties Data for Burning Natural and Synthetic Materials, Supplemental Report for National Bureau of Standards Project No. G8-9003, School of Aerospace Engineering, Georgia Institute of Technology, Atlanta, GA, May 1978.

Bankston, C.P., Zinn, B.T., Browner, R.F., Powell, E.A. 1981. Aspects of the Mechanisms of Smoke Generation by Burning Materials. Combustion and flame, volume 41, pages 273-292. Elsevier, 1981.

Beychock, M.R. 2005 Fundamentals of stack gas dispersion. Irvine, CA, 2005.

Bluett, J., Gimson, N., Fisher, G., Heydenrych, C., Freeman, T., Godfrey, J. 2004. Good Practice Guide for Atmospheric Dispersion Modelling. Ministry for the Environment, Wellington, New Zealand, 2004.

Beleids Ondersteunend Team Milieu (BOT-Mi). 2010. Brontermberekening concept 15 december 2010. Centrum voor Externe Veiligheid, 2010.

Beleids Ondersteunend Team Milieu (BOT-Mi). 2010. Effectberekening voor overige branden, concept 24 september 2010. Centrum voor Externe Veiligheid, 2010.

Beleids Ondersteunend Team Milieu (BOT-Mi). 2010. Info meteoklassen en wind. Versie Augustus, 2010. Centrum voor Externe Veiligheid, 2010.

Beleids Ondersteunend Team Milieu (BOT-Mi). 2010. Standaard veiligheidsafstanden voor PGS-15 branden, conceptversie 15 december 2010. Centrum voor Externe Veiligheid, 2010.

Briggs, G.A. 1969. Plume Rise. USAEC Critical Review Series, 1969.

Briggs, G.A. 1971. Some recent analyses of plume rise observation, Proc. Second International. Clean Air Congress, Academic Press, New York, 1971.

Briggs, G.A. 1972. Discussion: chimney plumes in neutral and stable surroundings., Atmospheric Environment, volume 6, pages, 507-510, 1972.

Butler, K.M., Mulholland, G.W. 2004. Generation and transport of smoke components. Fire Technology, volume 40, pages 149-176. Kluwer Academic Publishers, 2004.

- Campanelli, M., Delle Moanche, L., Malvestuto, V., Olivieri, B. 2003. On the correlation between the depth of the boundary layer and the columnar aerosol size distribution. *Atmospheric environment*, volume 37, pages 4483-4492. Elsevier, 2003.
- Chamberlain, A C. 1966. Transport of gases to and from grass and grasslike surfaces. *Proc. R. Sot. London, Ser. A*, 290, 236, 1966.
- Clough, W S. 1973. Transport of particles to surfaces. *Journal of Aerosol Science*, Volume 4, page 227, 1973.
- Committee for the Prevention of Disasters (CPD). 2005. Methods for the calculation of physical effects – due to releases of hazardous materials (liquids and gases) – ‘Yellow Book’, third edition, second revised print. CPD, 2005.
- European Environment Agency (EEA). 2009. Spatial assessment of PM10 and ozone concentrations in Europe (2005). EEA, Copenhagen, 2009.
- Ferin, J., Oberdorster, G., Soderholm, S.C., Gelein, R. 1991. Pulmonary Tissue Access of Ultrafine Particles. *Journal of Aerosol Medicine*, volume 4, pages 57-68. Liebert. 1991.
- Gad, S.C. 2005. Metals. *Encyclopedia of toxicology*, page 49. Elsevier, 2005.
- Gad, S.C., Gad, E. 2005. Polycyclic aromatic hydrocarbons (PAHs). *Encyclopedia of toxicology*, pages 513-515. Elsevier, 2005.
- Garcia-Perez, M. 2008. The formation of polyaromatic hydrocarbons and dioxins during pyrolysis: a review of the literature with descriptions of biomass composition, fast pyrolysis technologies and thermochemical reactions. Washington State University, 2008.
- Gifford F.A., 1961. Use of routine meteorological observations for estimating the atmospheric dispersion. *Nuclear safety Volume 2* pages 47-57.
- Graham, J.A., Gardner, D.E., Gardner, S.C.M., Miller, F.J. 2010. Toxicity of airborne metals. *Comprehensive toxicology: Chapter 8.21*, pages 405-420. Elsevier. 2010.
- Hertzberg, T., Blomqvist, P. 2003. Particles from fires - a screening of common materials found in buildings. *Fire and materials*, volume 27, pages 295-314. John Wiley & Sons. 2003.
- InfoMil. 2007. Handleiding PGS 15. InfoMil, Den Haag, 2007.
- International Commission on Radiological Protection (ICRP). 1994. Annual ICRP, volume 24, pages 1-482, 1994.
- Van Jaarsveld, J.A. 1995. Modelling the long-term atmospheric behaviour of pollutants on various spatial scales. Universiteit Utrecht, 1995.
- Van Jaarsveld, J.A. 2004. The Operational Priority Substance model: Description and validation of OPS-Pro 4.1. RIVM report 500045001, 2004.

Kennedy, I.M. 1997. Models of soot formation and oxidation. Progress in energy and combustions science, volume 23, pages 95-132, 1997.

Kreyling, W.G., Semmler, M., Moller, W.J. 2004. Dosimetry and Toxicology of Ultrafine Particles. Journal of Aerosol Medicine, pages 140-152, June 2004.

Leonard, S., Mulholland, G.W., Puri, R., Santoro, R.J. 1994. Generation of CO and smoke during underventilated combustion. Combustion and flame, volume 98, pages 20-34, 1994.

Levin, B.C., Kuligowski, E.D. 2005. Combustion toxicology. Encyclopedia of toxicology, pages 639-652. Elsevier, 2005.

Mackay, D. 1991. Multimedia environmental methods, the fugacity approach. Lewis Publications, Chelsea, MI, 1991.

Madl, A.K., Carosino, C., Pinkerton, K.E. 2010. Particle toxicities. Comprehensive toxicology: Chapter 8.22, pages 421-451. Elsevier. 2010.

Marine Accident Investigators International Forum (MAIIF). 2011. Available online: www.maiif.org/manuals , consulted on 2011-02-18. MAIIF, 2011.

Marx, J.D., Cornwell, J.B. 2009. The importance of weather variations in a quantitative risk analysis. Journal of loss prevention in the process industries, volume 22, pages 803-808. Elsevier, 2009.

Mastral, A.M., Callén, M.S. 2000. A review on polycyclic aromatic hydrocarbon (PAH) emissions from energy generation. Environmental science & technology, volume 34, number 15. American Chemical Society, 2000.

Van de Meent, D., De Bruin, J.H.M. 2007. Risk assessment of Chemicals: An introduction, Chapter 4 Environmental Exposure Assessment. Springer. 2007.

Mennen, M.G., Van Belle, N.J.C. 2007. Emissies van schadelijke stoffen bij branden, RIVM report 609021051. National Institute for Public Health and the Environment (RIVM), Bilthoven, The Netherlands, 2007.

Mennen, M.G., Kooi, E.S., Heezen, P.A.M., Van Munster, G., Barreveld, H.L. 2009. Verspreiding van stoffen bij branden: een verkennende studie, RIVM report 609022031. National Institute for Public Health and the Environment (RIVM), Bilthoven, The Netherlands, 2009.

Mohan, M., Siddiqui, T.A. 1998. Analysis of various schemes for the estimation of atmospheric stability classification. Atmospheric environment, volume 32, number 21, pages 3775-3781. Elsevier, 1998.

Möller, U., Schumann, G. 1970. Mechanisms of transport from the atmosphere to the earth's surface. Journal of Geophysical Res. , Volume 75, page 3013, 1970.

Mulholland, G.W. 2008. SFPE Handbook of fire protection engineering, 4th edition, chapter 2.13: smoke production and properties. Society of Fire Protection Engineers. National Fire Protection Association, 2008.

National Radiological Protection Board (NRPB). 1983. Models to allow for the effects of coastal sites, plume rise and buildings on dispersion of radionuclides

and guidance on the value of deposition velocity and washout coefficients. Report NRPB-157. NRPB, 1983.

National Radiological Protection Board (NRPB). 1986. NRPB emergency data handbook. Report NRPB-R182. Chilton, 1986.

Oberdorster, G., Oberdorster, E., Oberdorster, J. 2005. Environmental Health Perspectives, volume 113, pages 823-839. The National Institute of Environmental Health Sciences (NIEHS). 2005.

Richter, H., Howard, J.B. 2000. Formation of polycyclic aromatic hydrocarbons and their growth to soot- a review of chemical pathways. Progress in Energy and Combustion Science, volume 26, pages 565-608. Elsevier. 2000.

Roth, C., Scheuch, G., Stahlhofen, W. 1993. Clearance of the human lungs for ultrafine particles. Journal of Aerosol Science, volume 24, supplement 1, pages S95-S96, 1993.

Sehmel, G. A., Hodgson, W. H., Sutter, S.L. 1973. Dry deposition of particles. Pacific Northwest Laboratory Annual Report for 1973 to the USABC Division of Biomedical and Environmental Research, Part 3, Atmospheric Sciences. USAEC Report BMJL-1850 (Pt 3), page 157, Battelle Pacific Northwest Laboratories, NTIS, 1974.

Sehmel, G. A., Sutter, S. L. and Dand, M. T. 1973 Dry deposition processes. Pacific Northwest Laboratory Annual Report for 1972 to the USAEC Division of Biomedical and Environmental Research, Volume II, Physical Sciences, Part 1, Atmospheric Sciences. USAEC Report BKWL-1751 (Pt I), page 43, Battelle Pacific Northwest Laboratories, NTIS, 1973.

Seibert, P., Kromp-Kolb, H., Kasper, A., Kalina, M. Puxbaum, H., Jost, D.T., Schwikowski, M., Baltensperger, U. 1998. Transport of polluted boundary layer air from the po valley to high-alpine sites. Atmospheric Environment, volume 32, number 23, pages 3953-3965. Elsevier, 1998.

Seinfeld, J.H., Pandis S.N. 1998 Atmospheric Chemistry and Physics, from Air Pollution to Climate Change. John Wiley, New York, 1998.

Sijm, D.T.H.M., Rikken, M.G.J., Rorije, E., Traas, T.P., McLachlan, M.S., Peijnenburg, W.J.G.M. 2007. Risk assessment of chemicals: An introduction, chapter 3. Transport, accumulation and transformation processes. Springer. Dordrecht, The Netherlands, 2007.

Slinn, W.G.N. 1978. Parameterizations for resuspension and for wet and dry deposition of particles and gases for use in radiation dose calculations. Nuclear Safety, Issue 9, page 205, 1978.

Stec, A.A., Hull, T.R. 2010. Fire toxicity, 1st edition. CRC Press, 2010.

Tewarson, A., Jiang, F.H., Morikawa, T. 1993. Ventilation-controlled combustion of polymers. Combustion and Flame, volume 95, pages 151-169, 1993.

Turner, B.D. 1970. Workbook of atmospheric dispersion estimates. U.S. Environmental Protection Agency, No. AP-26, 1970.

Wesely, M. L., Flicks, B. B., Dannevik, W.P., Frisells, S., Husar, R.B. 1977. An eddy-correlation measurement of particulate deposition from the atmosphere. *Atmospheric Environment*, 11, page 561. 1977.

Witlox, H.W.M. 2010. Overview of consequence modelling in the hazard assessment package PHAST. DNV Software, 2010.

World Health Organization (WHO). 2000. Air quality guidelines: Chapter 5.9 Polycyclic aromatic hydrocarbons (PAHs). WHO Regional Office for Europe, Copenhagen, Denmark, 2000.

World Health Organization (WHO). 2010. Dioxins and their effects on human health, fact sheet N°225. WHO, 2010.

Young, R.A. 2005. Dioxins. *Encyclopedia of toxicology*, pages 70-72. Elsevier, 2005.